POSSIBLE TIMING OF THE TRANSITION FROM PRE-INDUSTRIAL TO INDUSTRIAL CLIMATE IN THE CENTRAL TO NORTHERN OF SWEDEN, BASED ON PROXY DATA FROM TREE-RINGS

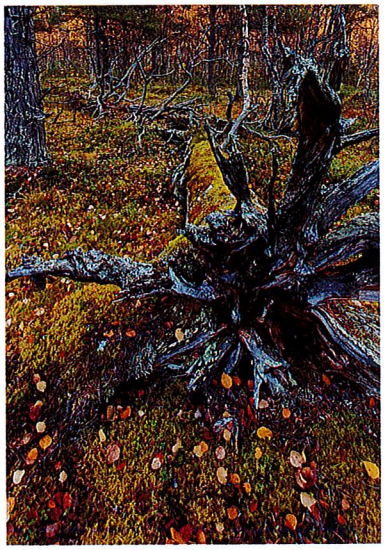

Mika Falkensjö Oppenheim

Degree of Master of Science (120 credits)
with a major in Environmental Science with specialization in Atmospheric Science, Climate, and Ecosystems
60 hec

Department of Earth Sciences
University of Gothenburg
2022 B1211

Faculty of Science

UNIVERSITY OF GOTHENBURG

UNIVERSITY OF GOTHENBURG
Department of Earth Sciences
Geovetarcentrum/Earth Science Centre

POSSIBLE TIMING OF THE TRANSITION FROM PRE-INDUSTRIAL TO INDUSTRIAL CLIMATE IN THE CENTRAL TO NORTHERN OF SWEDEN, BASED ON PROXY DATA FROM TREE-RINGS

Mika Falkensjö Oppenheim

ISSN 1400-3821

B1211
Master of Science (120 credits) thesis
Göteborg 2022

Mailing address
Geovetarcentrum
S 405 30 Göteborg

Address
Geovetarcentrum
Guldhedsgatan 5A

Telephone
031-786 19 56

Geovetarcentrum
Göteborg University
S-405 30 Göteborg
SWEDEN

Abstract

Earth's climate has varied through time, with orbital forcing as the most dominant force on the climate system the last million years, causing glacial-interglacial cycles. The last glacial period ended about 11.6 thousand years (kyr), ago and the last interglacial maximum around 6.5 kyr ago. A cooling trend towards a new glacial period followed, interrupted by the present human caused global warming, mainly due to burning of fossil carbon. The United Nations Framework Convention on Climate Change (UNFCCC) agreed upon the goal of the Paris Agreement 2015, with the aim of holding the increase in the global average temperature to below 1.5 – 2 ºC from pre-industrial temperatures. The Intergovernmental Panel on Climate Change (IPCC) has defined the pre-industrial baseline to values of 1850-1900 CE, a period when global emissions of greenhouse gases already had raised since the industrial revolution ca 1750 CE, and possibly already have had effects on the temperature.

The phenomenon of Arctic Amplification is a more pronounced warming in the Arctic region, with a present temperature rise of more than doubled compared to the global mean. Indications of an earlier transition from pre-industrial to industrial climate in high northern latitudes have been noticed and the aim in this thesis was to further explore this timing of the transition from pre-industrial to industrial climate in high northern latitudes. To do so, tree-rings have been used to reconstruct past temperatures.

Tree-rings provides a variety of proxies used for climate reconstructions, with the benefit of being easily accessed, well replicated and available in regions suitable for climate studies. In the Fennoscandian region, correlation between climate and tree-rings has proven to be good, which has led to an extensive tradition of dendroclimatology. Here, updated tree-ring width (TRW) and maximum latewood density (MXD) chronologies from Ammarnäs are presented, built from Scots Pine wood sources, living and dead (preserved on the ground). The MXD chronology was used as a base to investigate the timing of the transition to industrial climate.

The current warming could be detected and well defined in the updated MXD chronology from Ammarnäs. The warming rate of the present exceeded earlier warming rates throughout the chronology and a predominance of positive annual temperature anomalies could be seen between 1900 – 2021 (reference period 1971 – 2000), instead of the substantial predominance of negative annual temperature anomalies seen in all other centuries, except from the 16th century. A vague negative long-term trend represents the pre-industrial period, interrupted by a significant warming trend in the latest part of the chronology.

To further explore the time of transition to industrial climate in relation to latitude, three other sites in central to northern Sweden; Rogen, Jämtland and Torneträsk, were analysed. The timing of when the current warming started to emerge in the different data sets were decided by a change point analysis. This resulted in a latitudinal comparison, where a possible trend towards an earlier shift to industrial climate could be seen in the two more northern locations. The time of change was seen in 1916 in Torneträsk (68ºN), 1915 in Ammarnäs (66ºN), 1932 in Jämtland (63ºN) and 1929 in Rogen (62 ºN). This result does support the hypothesis of a possibly earlier transition to industrial climate in higher northern latitudes compared to lower, but the analysis contains few samples and would benefit from further replication.

Keywords: Tree-ring, maximum latewood density (MXD), Scandinavia, pre-industrial, industrial climate

Table of content

1. Introduction

1.1. Earth climate

The climate on Earth has been changing throughout its history because of natural fluctuation, both on longer and shorter time scales. During the Quaternary, the past 2.6 million years (Myr), glacial-interglacial cycles have influenced Earth's climate and since the middle of the Quaternary the frequency of these cycles has been about 100 thousand years (kyr), mostly influenced by Earth changes in its path around the sun, known as orbital forcing (Ruddiman, 2014; St John et al., 2012). The last glacial period come to an end around 11.6 kyr ago, as Earth entered the interglacial period of Holocene (Ruddiman, 2014). The climate come to stabilize and a slow cooling trend toward a new glacial period started around 6.5 kyr ago (Gulev et al., 2021; Masson-Delmotte et al., 2013). This trend was interrupted as the climate started to warm again, sometime after the industrial revolution, around 1750 CE, when human begun to burn fossil carbon in greater extent (Kaufman et al., 2009). The current warming is unequivocally a consequence of human activities on Earth, according to Working Group I (WGI) in the Sixth Assessment Report (AR6) from the Intergovernmental Panel on Climate Change (IPCC), and the rate of the present warming is rapid (Masson-Delmotte et al., 2021). The global mean temperature during the most resent decade (2011 – 2020) exceeds the warmest centennial-scale range reconstructed for the last interglacial, around 6.5 kyr ago, and the temperatures of today have not been present on Earth since ca 125 kyr (Masson-Delmotte et al., 2021).

Within the last 2 kyr variabilities in surface temperature have been estimated from climate reconstructions and the period is characterized as a stable period with a long-time cooling trend (Neukom, Barboza, et al., 2019), but periods of climate anomalies have occurred, such as the cool Little Ice Age (LIA) (1450 – 1850 CE) and the warm Medieval Climatic Anomaly (MCA) (950 – 1250 CE) (Masson-Delmotte et al., 2013). These periods of temperature anomalies identified during the last 2 kyr did not happen consistently as a global phenomenon, but rather as regional changes. In contrast, the modern warming is showing a distinct global pattern, both in spatial and temporal scale (Neukom, Steiger, et al., 2019).

The natural variability of Earth's climate needs to be taken in account when approaching changes in Earth's climate. Important external forcings, which all have been reasons to natural variability in Earth climate, are changes in Earth orbit around the sun and the tilt of Earth axis, volcanic eruptions, solar irradiance and changes in atmospheric composition (Masson-Delmotte et al., 2013). During the pre-industrial period 1300 – 1800 CE, volcanic aerosol forcing has, according to Neukom, Barboza, et al. (2019), been a main driver of multidecadal climate variabilities and the volcanic aerosol forcing is the strongest interannual force on the climate system, with greatest effects the first 3-5 years after a large eruption (Gulev et al., 2021). Furthermore, volcanic forcing does also influence slower components of the climate system, such as ocean surface temperatures, which have shown to have a slow recovery and therefore cause a long-term cooling effect as well (Broennimann et al., 2019). The warm MCA coincides with the Medieval solar maximum and was relatively free from large volcanic eruptions, whereas the cold LIA could have been triggered by massive volcanic eruptions in the 13th, and later sustained by further eruptions in the 17th and 19th centuries, in combination with the solar minim of Wolf, Spörer, Maunder and Dalton (Crowley & Unterman, 2013; Steinhilber et al., 2012). The Modern warm period is mainly caused by anthropogenic forcing on the climate system, due to emissions of greenhouse gases (GHG) and land use change, which have caused changes in the composition of the atmosphere and Earth's albedo (Masson-Delmotte et al., 2021). It also coincides with the Modern solar maximum and rather low volcanic activity

(Gulev et al., 2021). The current warming state is a consequence of the imbalance in Earth's radiative budget, as the added amount of GHG acts as a blanket, trapping heat in the atmosphere. However, sequences of volcanic eruptions during the early and mid-19th century, such as the Tambora eruption 1815 CE, make it hard to pinpoint exactly when the anthropogenic forced warming started to affect temperatures (Broennimann et al., 2019).

There are also internal drivers of the climate system, acting on different time scales, causing natural variance of the temperature. Important internal climate forcings with influence in the North Atlantic region and Scandinavia are the North Atlantic Oscillation (NAO), the Atlantic Multidecadal Variability (AMV) and the Atlantic Meridional Overturning Circulation (AMOC) (Gulev et al., 2021). The NAO can be described as a variation in atmospheric mass between the Arctic and the subtropical Atlantic (Hurrell et al., 2001), leading to changes in sea level pressure (SLP). Furthermore, this influences the strength of the Westerlies, which brings warm and moist air to the northern Europe (Wanner et al., 2001). During positive phases of NAO the westerly winds are strengthen (Linderholm et al., 2008; Linderholm et al., 2009). Negative phases of NAO are characterized by a weakening of the Westerlies, while cold weather from the Arctic and Russia are sweeping in over Scandinavia. The NAO is affecting the winter months most, but as a seasonal variability of the spatial pattern of SLP have been noticed the warm season is also affected. The NAO have influence on multidecadal-scale and have most likely not shown any unusual patterns in the instrumental record on a millennial or multi-centennial scale (Gulev et al., 2021). Further, the AMV is related to multi-decadal variability of the sea surface temperature (SST) in the North Atlantic, characterized by basin-wide warm and cold periods with an average variation of 0.4 °C of the SST (Gulev et al., 2021). But as the SST has risen steadily the last century and the paleo reconstructions of AMV are rather uncertain (Masson-Delmotte et al., 2013), there have been some uncertainties of the AMV signal (Gulev et al., 2021). But most likely, there has not been any anormal patterns of AMV during the instrumental period (Gulev et al., 2021). Accordingly, both NAO and AMV have multidecadal influences on the climate, causing variabilities between warmer and colder periods, but has most likely not caused any unusual fluctuations of the climate during the instrumental period. Furthermore, the AMOC is an ocean current, transporting heat from lower latitudes towards the northern parts of the Atlantic (Meredith, 2019; Rhein et al., 2013). It is driven by differences in density of the ocean water, due to temperature and salinity (Bindoff et al., 2019). This current acts as a heat engine, transporting warm water to the Artic region (AMAP, 2017). It influences the climate over land, and in the northern parts of Scandinavia this causes a milder climate then would have been expected otherwise. Indications of a weakening AMOC have been registered during the 21th century (Gulev et al., 2021), due to increased influx of freshwater, from increased melting of glaciers, caping the ocean and causing a less stratified ocean column (Bindoff et al., 2019).

Furthermore, the Arctic amplification (AA) is an important phenomenon in high latitudes concerning the climate. The AA is caused by a loop of several feedbacks triggered by the loss of ice and snow cover, causing lower surface albedo, which reduces reflected solar radiation (AMAP, 2017; Masson-Delmotte et al., 2013; Meredith, 2019). Furthermore, warm air holds more water vapor, which is a GHG, contributing to the amplification as well. At present time, the Arctic region surface temperatures have warmed three times as much than the global mean surface temperatures (AMAP, 2021). There is no single definition of the Arctic region, it can eg. be defined by the Arctic Circle (66.57°N) or a temperature isotherm. Other ways of defining the Artic can be based on landscape characteristics such as vegetation and treeline, permafrost distribution or by latitude, which can be misleading in some aspect, such as including areas without Arctic attributes. The Arctic Monitoring and Assessment Program (AMAP) uses some

definitions of the Arctic region which take into account physical, geographical and/or ecological characteristics (AMAP, 1998, 2022). Despite this, the definition in this thesis is 60 – 90º N, to be comparable to the reconstruction performed by Past Global Changes (PAGES) 2k Consortium (Abram et al., 2016; McKay & Kaufman, 2014; PAGES2k, 2022). This latitudinal definition of the Arctic region can be motivated eg. by having areas such as the southern parts of Greenland and Iceland included.

1.2. Statement of the problem

Accordingly, the temperature during the last 2 kyr experienced a slight cooling trend interrupted by the transition from pre-industrial to industrial climate (Kaufman et al., 2009). The concentration of CO_2 in the atmosphere has increased significantly, from ca 280 ppm to 421 ppm in June 2022 (NOAA, 2022), which is the highest levels in at least 2 Myr (Gulev et al., 2021). This unusual warming of the climate system is a large threat to life on Earth and according to IPCC special report "Global Warming of 1.5ºC" (SR1.5) there is a large risk for runaway effects and crossing of tipping points, which could cause unreversible damages to the climate system, if the warming caused by humans exceed +2 ºC from pre-industrial climate (Allen et al., 2018).

During the climate conference 2015 in France, the United Nations Framework Convention on Climate Change (UNFCCC) agreed on the goal of the Paris Agreement (PA), with the aim of "holding the increase in the global average temperature to well below 2 °C above pre-industrial levels and pursuing efforts to limit the temperature increase to 1.5 °C above pre-industrial levels". The carbon budget coupled to the PA include how much emissions humans have caused and how much there is left to emit to not exceed the goal of staying below 1.5 – 2 ºC. The remaining amount of carbon that can be emitted are strongly dependent on how the pre-industrial is defined. Therefore, it is highly important to get the base from when the warming started right, as every ton of CO_2 emission adds to global warming, where a near-linear relationship between cumulative CO_2 emissions and the increase of global surface temperature exists (Masson-Delmotte et al., 2021). The baseline will have an important impact on how future mitigation and climate goals are expressed, and further, on future global warming. The use of a pre-industrial baseline would preferably mean to use values of temperature that has not been influenced, or with as little influence as possibly, by human activities such as land use change and emissions of GHG. It is also desirable to use a period which is close to, or similar to present days external forcings (Hawkins et al., 2017). The IPCC report AR6 (WGI) uses 1850 – 1900 CE as an arbitrary baseline, representing pre-industrial temperatures, but there is a large risk of missing some of the human enhanced warming if defining pre-industrial too late (Schurer et al., 2017).

There is also a large risk of missing the true timing of this transition as the suggested period of the pre-industrial is based on global reconstructions, but with areas as e.g. the Arctic left out (Schurer et al., 2018). As the AA makes the Arctic extra sensitive to surface temperatures, and already displays a pronounced warming at present time (AMAP, 2017; Meredith, 2019), this region might also have responded earlier to the anthropogenic warming. In analyses and simulations performed by Abram et al. (2016), the Arctic region were showing the transition towards a warming climate earlier than other land areas, indicating that regionally differences must be sufficiently investigated. To further strengthen the point of a reginal approach to the problem, Neukom, Steiger, et al. (2019) stated that climate reconstructions from the last 2 kyr have shown a lack of globally coherence in warm and cold periods during the pre-industrial period, as forcings probably was not sufficiently enough to cause globally synchronous extreme

temperatures. The ongoing global warming on the other hand is the warmest period of the last 2 kyr for more than 98% of the globe (Neukom, Steiger, et al., 2019).

1.3. The aim and objectives

The aim of this thesis is to define the timing of the transition from pre-industrial to industrial climate in locations representing a latitudinal climate gradient throughout the central to northern Sweden. Further, as the Arctic is extra sensitive to climate change, because of the AA, the hypothesis is that the transition from pre-industrial to industrial climate could have emerged earlier in this region in comparison to a global scale.

To examine the timing of change to industrial climate, temperature reconstructions based on tree-ring proxies from Scots Pine (*Pinus Sylvestris L.)* are used. Further, Ammarnäs, located in the Swedish part of the Scandinavian mountains, are used as a key site. The goal is to update an existing tree-ring chronology from Ammarnäs, to improve the data and use the temperature reconstruction as the basis for the analysis of the timing of change from pre-industrial to industrial climate. This also include the secondary aim, to contribute to higher spatial coverage of high-quality climate reconstructions in this region.

Further, to enable the investigation of a possible spatiotemporal pattern regarding the time of the transition to industrial climate in high northern latitudes, data from Ammarnäs is compared to temperature reconstructions based on tree-ring data from Torneträsk, Jämtland and Rogen. Furthermore, all used sites in this thesis are located above 60º N to be representative of the Arctic region, as defined in this thesis.

2. Tree-rings and climate

2.1. Reconstructing past climate and climate proxies

The records of instrumental observed meteorological data of temperature and precipitation are too short to discover climate changes on timescale larger than multidecadal, and it does not cover the entire period of interest for this thesis. Instrumental data only go back to the beginning of the 19th century and reconstructions of past climate from natural archives, such as ice cores, tree-rings, ocean sediments and speleothems, are a way to expand our knowledge of past climate further back in time.

There is of cause some potential problems when using proxy data and creating reconstructions of past climate. For example, to know the accuracy of the reconstruction, which can be tested against other archives, proxies, reconstructions, and instrumental data, to investigate the potential of the reconstruction. Tree-rings, the archive used in this study, usually suffer from the disadvantage of not being able to capture centennial- to multicentennial-scale temperature variabilities, because of the shortness of each individual indices and the method of detrending by removal e.g. biological age effects (Esper et al., 2013; 2016). On the other hand, it is often easy to assess, well replicated and have shown the possibility to obtain a strong climate signal.

2.2. Dendrochronology and dendroclimatology

The science of dendrochronology, a dating method based on the width of tree-rings, was developed during the beginning of the 20th century. Dendroclimatology, a subfield of dendrochronology that cover the interest of this thesis, stands for the study of present and past climate based on information obtained from annually growing tree-rings (Speer, 2010).

In trees growing in areas with pronounced seasonality, a new growth ring is produced each year. The change in seasons causes variability in growth speed and results in different wood density throughout the yearly produced growth bands. The early growth (earlywood) produces a light-coloured tissue, consisting of large cells with thin cell-walls, while the tissue grown later in the season (latewood) is darker with smaller cells and thick cell-walls. There is a gradual transition between early and latewood, but a visible contrast exists between the two periods because of their difference in wood density. Boundaries between rings from different years are more clearly seen, as the latewood growing phase ends with small dark rings as the tree enter the dormant phase during the winter, and when the growth starts in the spring the cells are light and big again (Fritts, 1976; Speer, 2010).

2.3. Tree-ring data

The tree-ring width (TRW) is the most commonly used proxy in dendrochronology and the width of a year band is a consequence of the impact from the limiting factors of growth in the environment the tree lives in. Climate is one factor that can limit the growth of a tree, where temperature usually is the limiting factor close to the altitudinal or latitudinal treeline, while precipitation is the limiting factor in arid areas (Speer, 2010). Further, TRW is influenced by other signals than climate, e.g. stand dynamics, disturbances such as fires or insect infestations etc. These signals are referred to as noise, as it interferes with the wished-for climate signal, and with the aim to remove this noise, detrending of the data is necessary (Fritts, 1976; Speer, 2010). The benefit of TRW measurements is that it is relatively easy to obtain, cost-effective and it has shown a good correlation to parts of the growing season temperatures in trees grown at locations with extreme climate conditions.

Another proxy from the annually growing tree-rings is the maximum latewood density (MXD), which has shown the benefit of being more climate sensitive than TRW (Linderholm et al., 2010). Furthermore, MXD have shown a higher correlation to growing season temperatures in Scandinavia, with less noise disturbing the climate signal than seen in TRW (Gouirand et al., 2008), but detrending the data is still necessary to remove biological (non-climatic) trends. On the other hand, MXD measurements is more time consuming, requires specific and highly expensive instruments and knowledge to measure, but can be seen as a superior temperature proxy compared to TRW alone (Ljungqvist et al., 2020).

2.4. Dating of tree-rings and chronology building

The method of dating starts with counting the rings, from the bark towards the pith and as the outmost ring can be dated to the year it was sampled, if the growing season had started, an absolute dating can be attained to this year. The rest of the rings can be dated in relation to that year and later tested against other samples to be able to be confident about the accuracy of the dating throughout the sample (Fritts, 1976; Speer, 2010).

The way to test the dated samples is the practice of cross-dating, which consists of matching the pattern of wide and narrow rings between different samples. This provides the possibility

to find errors and mistakes within the counted samples and will serve as a quality control providing the possibility to control the absolute dating of each ring. The principle of cross-dating suggests that the variation in width of the rings is caused by growth limiting factors in the environmental of the tree (Fritts, 1976; Speer, 2010). As trees grow there is a risk that false rings are produced when the limiting factor of growth in the area is starting to slow the growing, but then better conditions for a continuous growing season is coming back. For example, if temperature is the limiting factor and the temperature gets really cool during the summer, the growth starts to slow down, and the latewood will start to be produced. Eventually the summer gets warm again and the structure of earlywood will be what is produced again. This will cause a visually "false ring". On the other hand, some years the growth is extremely limited, and no growth take place at all in some samples, or a ring can be locally absent in a tree. The absent of a ring is often called a missing ring. Hence, cross-dating is a way of discovering false and missing rings, as these most likely will not be the same in all samples (Fritts, 1976). As the cross-dating starts, the most easily dated samples are tested against each other first, with the aim to create a reference of the ring pattern. Often narrow rings are used as "pointer years" and then problem areas can be fitted in between and hopefully can false or missing rings be detected (Speer, 2010).

From the cross-dated samples a master chronology is built, preferably with samples from at least 20 trees and two sampled radii from each tree. The sample depth in different parts of the chronology varies, especially when using both living and dead threes, usually with a greater depth closer to the present. Periods of lower replication need at least a sample depth of five samples to be parts of the chronology, and preferably more to be trustful.

When building longer tree-ring chronologies, including relics of drywood (dead wood preserved standing or lying on the ground), samples with unknown age needs to be fit into the chronology. Old remnants of wood, drywood, from Scots Pine can be preserved up to thousand years in right conditions (Linderholm et al., 2014), which leads to demanding and time consuming work to accurately date the old wood. This is done by using cross-dating again, and possibly finding a time period with good correlation between the sample and the existing chronology. This must be done with caution and the sample should fit well both visually and statistically. Further, this enables the old sample to be dated to exact calendar year. Some samples are too old to overlap with the existing chronology, possibly matching with other samples, together creating a floating chronology with unknown age.

3. Data and method

3.1. Study area and sample site

The sampling site (66°06 N 16°20 E), is located ca. 10 km northwest of Ammarnäs, in the County of Västerbotten, Northern Sweden (Fig. 1). The site lies on the boarder to Vindejfjällens Natural Reserve, on the eastern side of the Scandinavian Mountains, with maritime climate to the west and continental climate to the east. The high peaks on the Norwegian side of the mountain range are subtracting much of the moist out from the damp sea air from the Nort Atlantic Ocean, and the climate in Ammarnäs is continental with maritime influences.

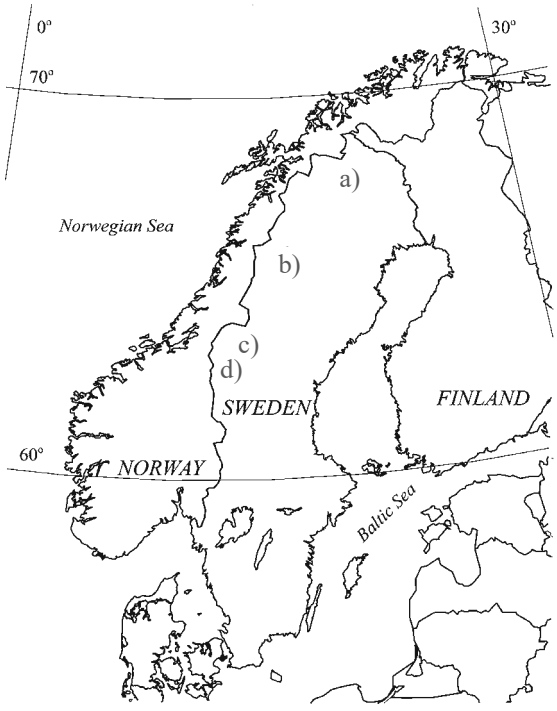

Figure 1. Map showing the location of the sampling site Ammarnäs and the locations used for comparing the timing of a detectable current warming trend. a) Torneträsk, b) Ammarnäs, c) Jämtland and d) Rogen

Further is the climate in Ammarnäs temperate and cool, with mean monthly temperatures of -10.9 ºC in January and 13.1 ºC in July during the Normal period 1971 – 2000 (most recent data available for Ammarnäs at SMHI) and mean annual precipitation of 655 mm (Fig. 2) (SMHI, 2022a).

The area is located around 70 km south of the Polar Circle. The formerly glaciated landscape displays steep southeast- and gentle northwest-facing slopes and a surrounding with rather smooth and rounded peaks (Fig. 3a), reaching 1400 – 1800 m above sea level (a.s.l.).

The vegetation of the sampling site consists of typical species close to the altitudinal treeline (ca 650 m a.s.l.) in this region such as mountain birch (*Betula pubescens var. tortuosa*), dwarf birch *(Beluna Nana)* and different types of shrubs (e.g. *Salix lapponum*) (Fig. 3a & 3b). Forests of Scots Pine, as at the sample site, are rather rare in this region.

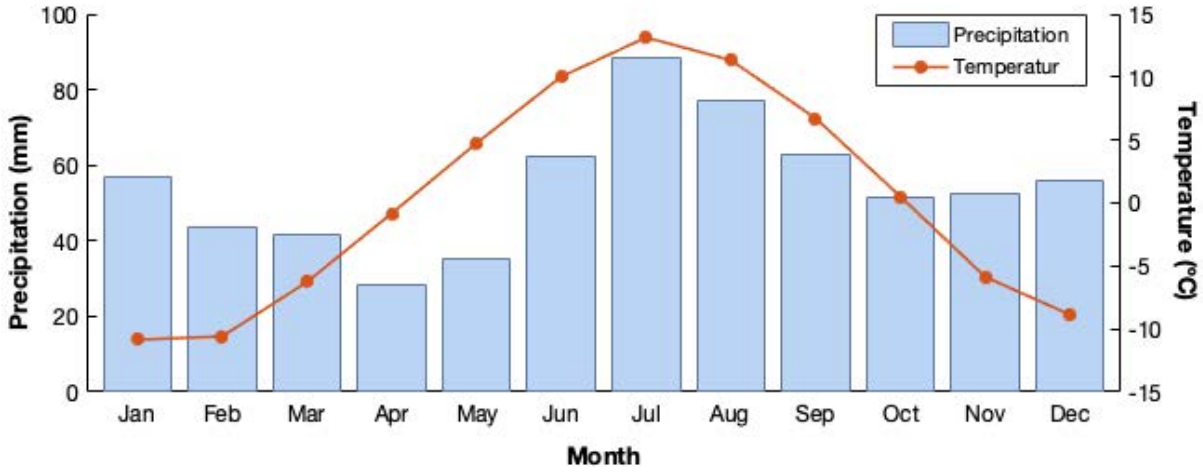

Figure 2. Monthly mean precipitation (1971 – 2010) and temperature (1971 – 2000) in Ammarnäs (SMHI, 2022a).

3.2. Fieldwork

All samples were collected by the principal investigators Björn Gunnarsson and Hans Linderholm. The old data was sampled 2010 and the new data was sampled 2021, by standard sampling methods of dendrochronology (Stokes & Smiley, 1996), in an elevation gradient along a south facing slope, between ca 500 - 650 m a.s.l., the approximate treeline. Altogether samples from 133 trees have been sampled in Ammarnäs, 80 from living trees and 53 discs/pieces of drywood, Table 1 shows how many that were used in the final updated chronology.

From the living trees, two radii from each tree were drilled (Fig. 3c), with some exceptions, with a 10 – 12 mm Swedish increment borer (from Haglöfs), at chest height (ca 1.3 m above ground). The drywood samples were sawed in ca 5 cm discs (Fig. 4a), samples taken approximately 1.3 m above the root collar, with some exceptions depending on the condition of the wood. The pieces of drywood were packed and stored in plastic bags to prevent the wood from drying too much (Fig. 4b).

Figure 3. a) View of the mountain landscape, b) the typical landscape of the sampling site, with birch and Scots Pine, in the fore field a standing tree of drywood can be seen, and c) drilling of a living trees, sample taken at "chest height" ca 1.3 m above the ground

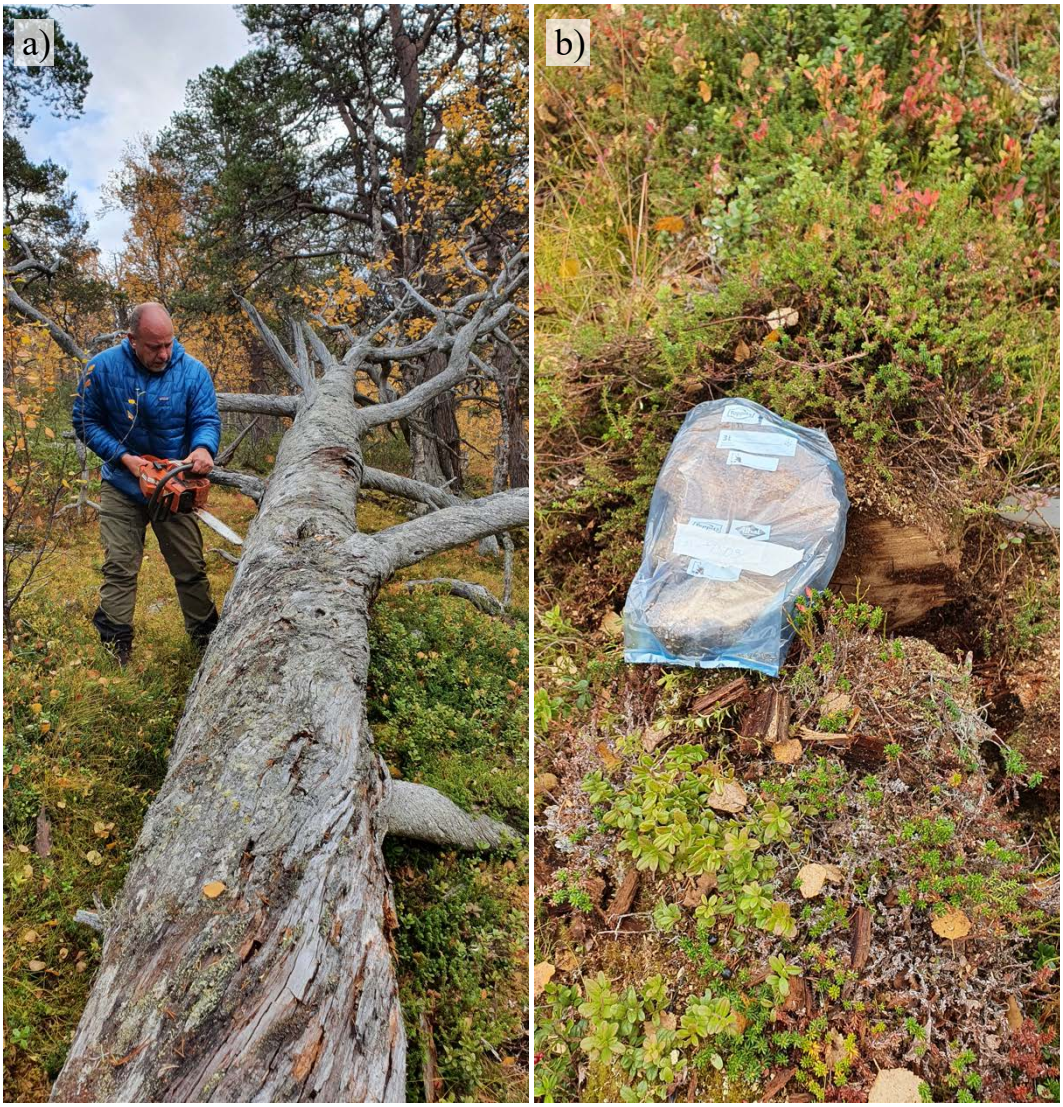

Figure 4. a) Björn Gunnarson cutting a large drywood Pine with chine saw and b) a disc of drywood packed up in a plastic bag for storage.

Table 1
Data used in the updated Ammarnäs chronologies. The new data is sampled 2021 and the old 2010. MSL = mean segment length.

Data	Wood typ	Samples	First year	Last year	MSL
New data	Living	53	1695	2021	138
	Drywood	17	1010	2016	161
Old data	Living	25	1629	2010	242
	Drywood	35	1277	1989	182

3.3. Preparation and measurement of TRW

The core samples from living trees were prepared accordingly to standard dendrochronology techniques for TRW measurement (Stokes & Smiley, 1996). Further, the samples from living trees were glued on a 10*10 mm wooden stripe, to protect and prepare them for the sawing required for the MXD measurement (Fig. 5a). Then they were grinded with gradually finer sandpaper, down to P800, which made the wood nicely polished with clearly seen cells. On the discs and pieces of drywood the 2 – 3 most desirable radii were polished and measured in the same way as the living trees. To prepare the wood for the twin blade saw, it was cut in 1.5 * 1.5 cm pieces along the chosen radii (Fig. 5b & 5c).

Annual ring-width measurement were accomplished by measuring each radii from the bark towards the pith, along the axis of the cell structure. This was done by using a stereomicroscope, with the accuracy of +/-0.001 mm, connected to a measurement table "LINTAB 5" and the Time Series Analysis Program (TSAP), software from Rinntech (Rinntech, Heidelberg, Germany). The two samples from each tree were measured and a visual comparation in TSAP followed. The correlation between the two samples were further examined by preforming a crossdating in TSAP and if the values were satisfying a mean of the trees were created. Later all trees mean values were crossdated towards each other and adjustments were done when false or missing rings were detected. When all trees were crossdated, a final check in COFECHA (Holmes, 1983) were done to ensure all rings were accurately dated with the right calendar year.

3.4. Preparation and measurement of MXD

The measurement of MXD were done by using the ITRAX wood scanner (Cox Analytic Systems) at the tree-ring laboratory of Stockholm University. Laths with a thickness of 1.2 mm (Fig. 5d) were sawed by using a twin saw (Fig. 6a). The thin laths were then put in the Soxhlet apparatus (Fig. 6b) with pure alcohol for ca 24 h to extract resins and other compounds. Afterwards the laths were dried from the alcohol and acclimatised in a room with controlled temperature (20 ºC) and air humidity (50%), yielding a 12% wood moister content. The samples were mounted and placed in the ITRAX scanner (Fig. 6c), where they got exposed to a narrow, high-energy, X-ray beam. The chrome tube in the scanner was turned to 30kV and 50 mA, with 75 ms step-time and the sensor slit was set to be open for 20 µm at each step. From the sensor, a 16-bit, greyscale, digital image with a resolution of 1270 dpi was produced. By using a calibration wedge with known density provided by Walesch Electronics the grey levels of the greyscale image were calibrated against values of wood density (Linderholm & Gunnarson, 2019).

The radiographic pictures of each radii were measured in WinDENDRO (Regent Instruments inc.), to obtain the MXD values and a mean for each tree were created. The mean values were double checked in CHOFECHA, and when the measurements were proven to be correct the samples were ready to be detrended.

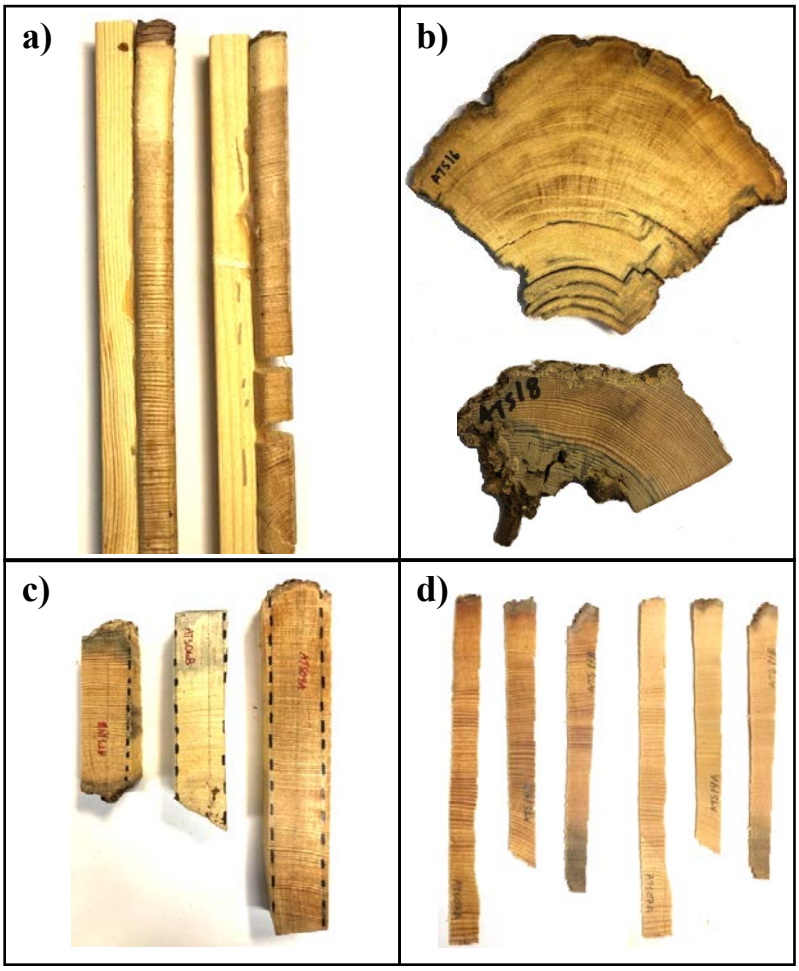

Figure 5. Pictures taken of a) cores from living trees, b) drywood samples, c) drywood samples prepared for the twin blade saw, and d) ca 1.2 mm thick laths prepared for x-ray, in the three darker samples to the left, the resin has not yet been subtracted, as it has in the lighter samples to the right.

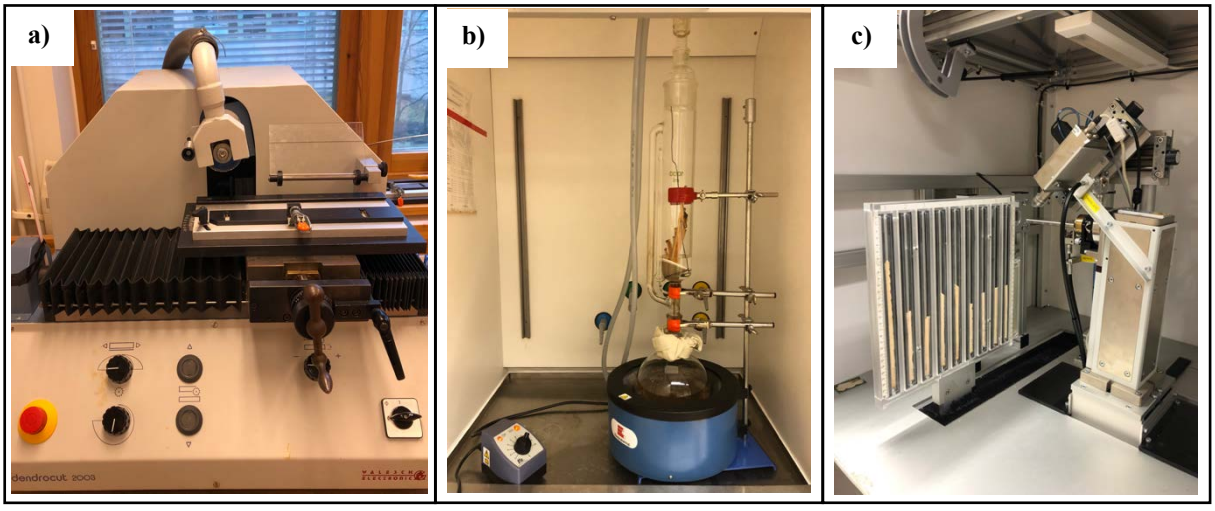

Figure 6. a) the twin blade saw used to produce the laths b) the Soxhlet apparatus used for restraining resin and other compounds from the wood and c) inside the ITRAX multi scanner showing a frame containing laths prepared for radiometric measuring.

3.5. Standardization

To obtain the climate signal and remove the undesired non-climatic (biological, e.g. age or stand dynamics) effects, the raw TRW and MXD data were standardized, with the aim to preserve as much low-frequency information as possible. The age dependant growth trend was the main signal to be removed, with the aim to create dimensionless indices suitable to use as climate proxies. A regional curve standardisation signal free method was applied on both the TRW and MXD data (Linderholm & Gunnarson, 2019; Melvin & Briffa, 2008). The non-climatic trends were removed by fitting a smoothing spline with 51 years stiffness to the data by using the Ssig Free software program (Cook et al., 2014 , software available at https://www.ldeo.columbia.edu/tree-ring-laboratory/ resources/software). The smoothing spline acts as a low-pass filter and removes the undesired biological trends in the wood, the stiffness of the spline (here 51 years) decides how flexible the spline is (Helama et al., 2004). For further insight of chosen method see Linderholm and Gunnarson (2019). The RCSig Free program did also build the chronologies from the detrended data.

3.6. Meteorological data

To investigate the possible timing of the transition from pre-industrial to industrial climate, there was a wish to use the tree-ring proxy data to reconstruct past temperatures. Hence, temperature data from nearby meteorological stations were examined, with the desire to use for the reconstruction.

Available meteorological data from Ammarnäs only spans over ca 30 years (1971 – 2000). On the other hand, data from Stensele, ca 10,5 km from Ammarnäs, provided instrumental temperature measurements for 144 years (1861 – 2004). The correlation (R) between the two data sets is very strong (R = 0.997) and the data from Stensele can be seen as representative of Ammarnäs.

3.7. Temperature reconstruction

To investigate the temperature signal in the TRW and MXD data the correlation between the observed data from Stensele and the proxy data were examined (Fig. 7). Both correlations to individual month and different warm seasons periods were tested against the data, to find the best correlations for further temperature reconstruction.

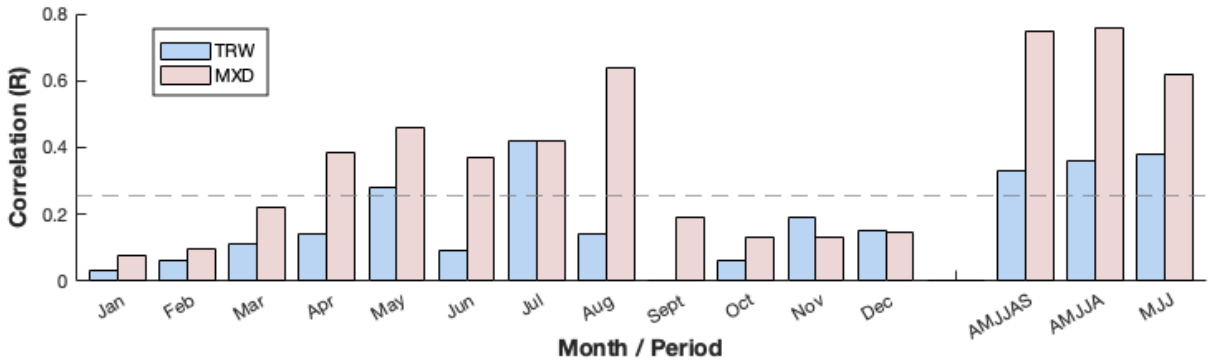

Figure 7. Monthly and seasonal correlation (R) between observed temperature data from Stensele and TRW and MXD over the period 1861 – 2004. The striped line represents the value of significant correlation for p>0:01 level. AMJJAS = April – September, AMJJA = April – August and MJJ = May – July.

For the temperature reconstructions a transfer models were designed based on the association between the indices and the metrological observations, where the observed temperature was set as the predictand and the proxy data as the predictor. The split sample calibration-verification procedure was used, where the full period of overlapping meteorological observations and proxy data (1861 – 2004) was split in two periods of equal length. When 1933 – 2004 was used for calibration, 1861 – 1932 was used for verification and vice versa. The calibration and verification statistics were calculated for the first and second period respectively. To validate the models, statistics of explained variance (R^2), reduction of error (RE), coefficient of efficiency (CE) and mean square error (MSE) were calculate (National Research Council, 2006). A sign test was also performed for each reconstruction, showing the agreement and disagreement in two data sets. When the results were satisfying, final models were calibrated over the full period of 1861-2004 and a temperature reconstruction was created.

The uncertainty was estimated of both the reconstruction and the chronology data. The standard error (SE) represented the uncertainty of the chronology, based on the replication through time (Yang et al., 2014), and the uncertainty associated with the reconstruction were estimated by the root square mean error (RMSE) statistic (Cook et al., 1999).

To compare different data sets towards each other, normalization (Z-score) was used, to make this easier. In most cases this was done in relation to the mean of the period 1971 – 2000, creating temperature anomalies to this reference period. The latest normal period for meteorological observation (30-yrs) is 1991 – 2020 (SMHI, 2022b; WMO, 2022). Further, for climate comparison the period 1961 – 1990 are most commonly used, with recommendations from The World Meteorological Organization (WMO, 2022). The chosen reference period in this thesis, 1971 – 2000, was decided upon as the last available data from Ammarnäs was for this normal period and the data used for the reconstruction were available until 2004 (SMHI, 2022a).

3.8. Change point analysis

To decide the timing of when the current warming was statistically detectable in the data sets an analysis with the ability to find a significant change in trend was desired to use. Change points are abrupt changes in times series and may represent transitions between different states within the data. Change point analysis has successfully been used within the area of climate change before (Aminikhanghahi & Cook, 2016).

Hence, a change point analysis was used with a segmentation approach (Aminikhanghahi & Cook, 2016; MathWorks, 2022). This analysis provides an investigation of the timing of a change by dividing the data in two regions of different mean values. The change point is set to the index value that will minimizing the sum of the residual errors of each region from its local mean value (MathWorks, 2022). The analyses were performed in MATLAB, by the script of "findchangepts" (MathWorks, 2022).

4. Results

4.1. The updated Ammarnäs chronologies

The updated TRW and MXD chronologies from Ammarnäs (Fig. 8) consist of 78 living cores and 52 drywood samples (*n=130*), from Scots pine, collected in 2010 and 2021. The updated chronologies were expanded back in time, from 1277 to 1010 CE, but the sample depth is low in the earlier parts and reaches a stable bas of 5 samples at 1511 CE, which is seen as the minimum number of samples for a reliably segment of a chronology.

The intercorrelation of the TRW chronology is 0.601 and the MXD chronology 0.692, a value representing the strength of the signal common for all included trees. This signal varies between all samples and should be at least 0.4 to be reliable for cross-dating. The variability of the width of rings from year to year is expressed as the mean sensitivity, this value should preferably be between 0.2 – 0.4 to be used in climate reconstructions (Speer, 2010). The mean the sensitivity of the TRW chronology is 0.204 and for the MXD 0.141.

In Fig. 8, the two chronologies are plotted together, showing rather similar variability from the 14th century until present. The TRW data show larger variance, especially around 1500 and 1600 CE, compared to the MXD data. The period before 1300 CE, when the two proxies are less harmonized, suffers from low sample depth and the expressed population signal (EPS) are well below the threshold of being reliable, for both TRW and MXD. The EPS represents the reliability of a chronology through time, this quantifies the number of trees needed in the chronology in order to be representative for the whole stand and the threshold of a reliably EPS is >0.85 (Wigley et al., 1984). The EPS value of the MXD data are slightly better than for TRW throughout the full time period, but both chronologies reach a stable EPS>0.85 in 1511 CE and stays above the threshold until present time.

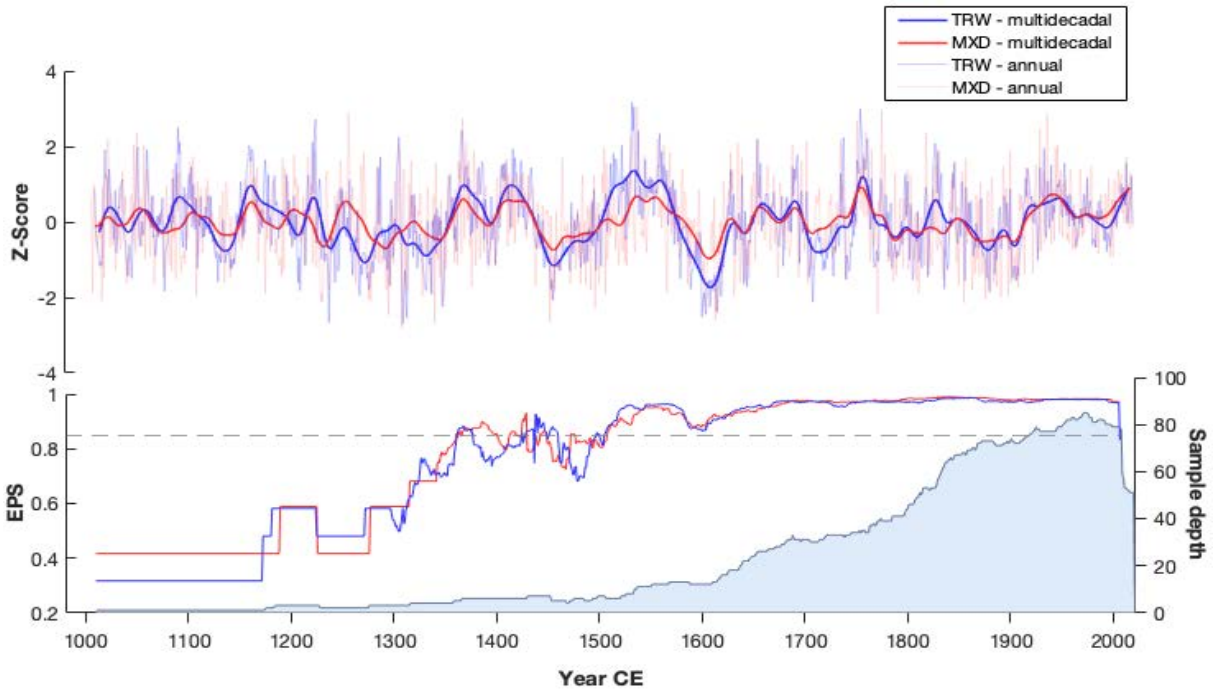

Figure 8. Normalized values over the full period of the updated TRW and MXD chronologies, showing annual and multidecadal variability (smoothed by a 30-year gaussian filter). TRW is represented by blue lines and MXD by red, also in the lower figure as EPS values, the striped line represents an EPS value of 0.85 and the blue coloured area the sample depth trough time.

As the correlations to the instrumental data was pronouncedly better for the MXD data than for the TRW data (Fig. 7), the main focus has been on the MXD data. Therefore, a more detailed description of the updated MXD chronology will follow.

In Fig. 9, the MXD data from Ammarnäs are compared between the old (sampled 2010), new (sampled 2021) and total data (all samples). There are mostly similar trends seen in variance, but the amplitude of the variability differs between the three data sets. The new and total data show more common variations in the latest part of the chronologies, 1950 – 2021 CE, while the old and total data shows more common pattern between 1500 – 1950 CE. In the earliest section the variance is most common between the new and total data. These trends are related to sample depth in respective data set (Fig. 9) and the dominance in the chronology of the total data. The new data shows a variability of lower amplitude than the old data.

The EPS value is sustained above the threshold 0.85 from 1511 – 2021 CE in the updated MXD chronology (Fig. 11) and from 1513 – 2010 CE in the old data (Appendix 2). In the updated version, the EPS is also above or close to 0.85 from 1364 – 1511, which is an improvement from the old data where the EPS drops substantively before 1513.

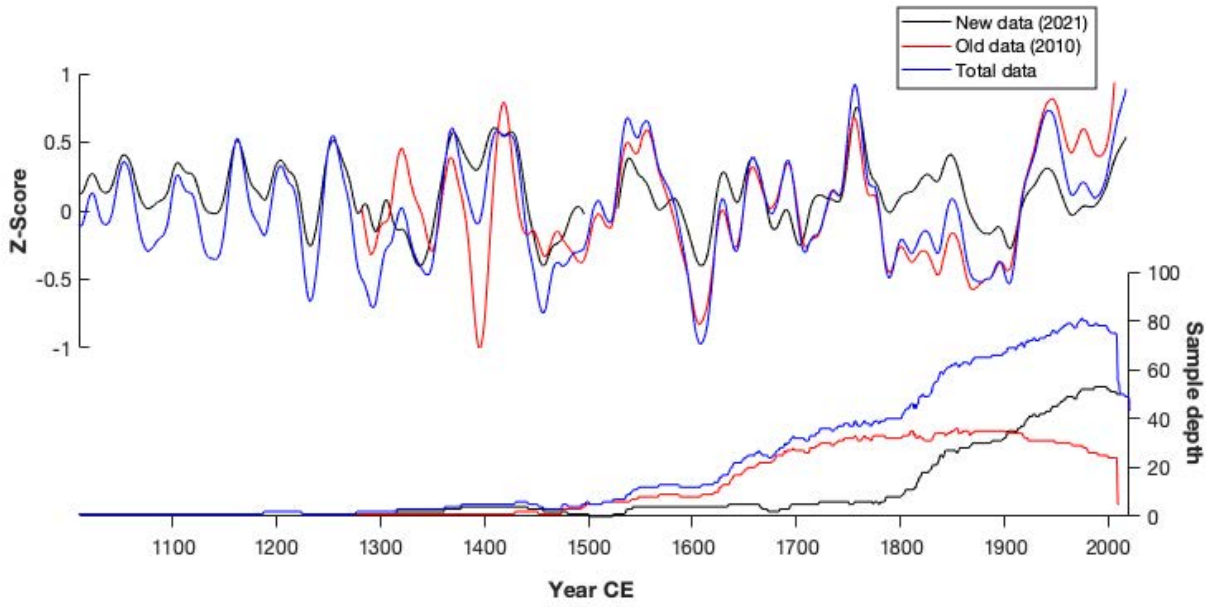

Figure 9. A comparison of the new (2021), old (2010) and total MXD data from Ammarnäs, normalized over the full period and smoothed by a 30-year gaussian filter. Sample depth below, representing the data with the same colour.

4.2. Climate reconstruction

The MXD data showed significant correlation to April – August temperatures, while the TRW data only showed significant correlation to May and July temperatures (Fig. 7). On the other hand, both MXD and TRW did show significant correlation to all three seasonal periods. But as the MXD data showed pronouncedly better correlation to the observed temperatures, a temperature reconstruction was only created based on the MXD data. In Appendix 4, the spatial distribution of the correlation between the MXD data and gridded data from CRUTEM 4.6 can be seen.

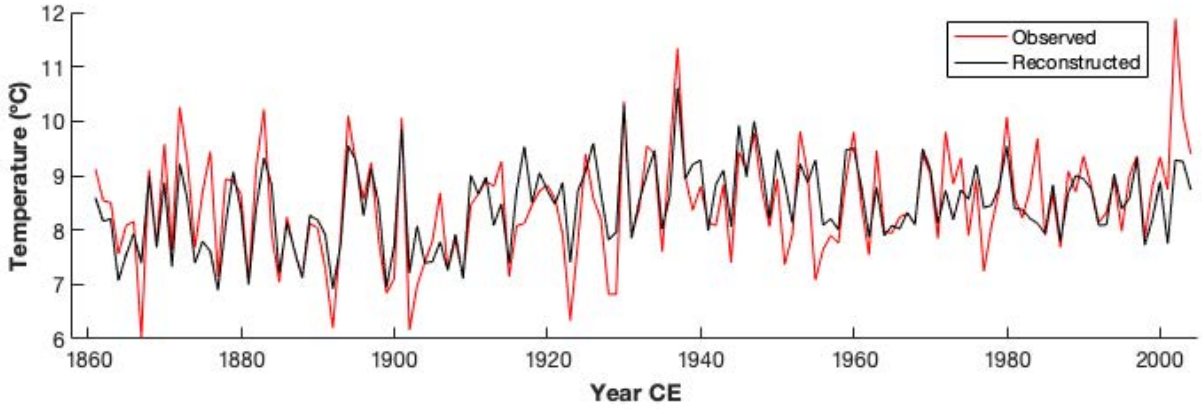

Figure 10. Comparison between observed, April – August, temperature data from Stensele and reconstructed temperature, of the same period, based on MXD data, showing a correlation of R = 0.76 and 57% of the variance in the observed temperature can be explained (R^2 = 0.57).

Hence, the updated MXD chronology from Ammarnäs correlated well with the instrumental record of April – August temperatures from the close lying metrological station in Stensele (R=0.76) (Table 2, Fig. 7 & 10). In Fig. 10, the observed and reconstructed temperature data are plotted against each other, showing similar patterns in variance and overall trends, and in Fig. 11, the temperature reconstruction, of April – August, from the MXD data can be seen. The temperature reconstruction was able to explain 57% of the variance in observed temperatures (Table 2). This was an improvement from the old data from Ammarnäs, which only could explain 51% of the variance (Appendix 3). Furthermore, the statistics regarding the relation between observed data and the different MXD data shows the strongest correlation to the new data and the weakest to the old (Appendix 3). The calibration-verification statistics displays the same, the new data alone shows the best fit to the observed data, where 61% of the variance in the observed temperatures could be explained, while the old data only can explain 51% of the variance and the total data 57% (Table 2 & Appendix 3).

Table 2
Calibration and verification statistics of the April – August temperature reconstructions from the updated (total) MXD data from Ammarnäs.

	Ammarnäs MXD SSF chronology		
Calibration period	1861-1932	1933-2004	1861-2004
Correlation, *R*	0.78*	0.67*	0.76*
Explained variance, R^2	0.61	0.45	0.57
Observations	72	72	144
Verification period	1933-2004	1861-1932	
Explained variance, R^2	0.45	0.61	
Reduction of error, *RE*	0.59	0.69	
Coefficient of efficiency, CE	0.44	0.61	
Mean square error, MSE	0.43	0.40	
Sign test +/-	61/9*	60/11*	

**Correlation is significant at the $p < 0.01$ level*

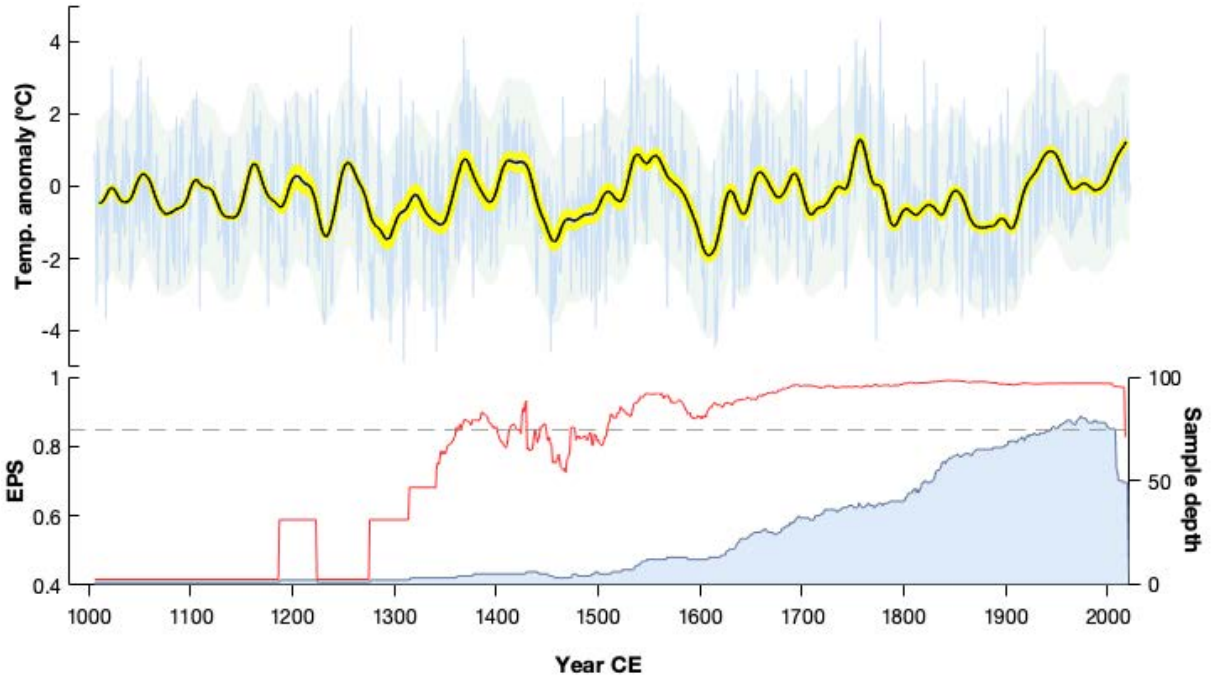

Figure 11. The updated Ammarnäs MXD based warm-season (April - August) temperature reconstruction, given as anomalies relative to the 1971 – 2000 mean. The thin blue line shows annual-variability and the black line the multidecadal variability (Gaussian filter, 30 years smoothing). The thick yellow line represents +/- 2 standard errors of the MXD chronology, and the green shaded area +/- 2 root mean square errors based on the calibration period. EPS and sample depth values below, the striped line represent an EPS value of 0.85.

A slight negative long-term trend can be seen in the pre-industrial part of the reconstruction and a pronounced positive in the later part (Fig. 12). Before the 20th century, the April – August temperatures have been more below than above the 1971 – 2000 average (Fig. 12), but in the mid-14th to mid-15th, possibly the MCA, 16th and 18th centuries the reconstruction shows rather pronounced, but shorter warming events, with temperatures close to the present. The cold LIA could possibly be seen between ca 1600 – 1750 CE or ca 1780 – 1900 CE.

Cooler periods have been more sustained than the warm once, with longer periods of negative temperature anomalies than positive. The longest sustained period of negative anomalies is 1599 – 1612 (14 years T = 9.09 ºC) and the longest period of positive anomalies is 1549 – 1559 (10 years T = 7.69 ºC). From 1511 – 1899 CE negative anomalies are predominant in the annual data, but for the 20th century and onwards a shift can be seen to a predominance of positive anomalies. From 1893 CE positive annual anomalies dominates all 50 years periods until present day (Fig. 12 & Table 3).

The period 1900 – 2021 CE were the warmest century throughout the chronology (mean T = 8.64 ºC), further were the latest hundred years (1922 – 2021) warmer (T = 8.73 ºC) and the latest 50 years were even warmer (8.94 ºC). The period 1900 - 2021 shows the largest rate of change with a warming of +0.04 ºC/decade compared to the mean temperature of the 19th century (mean T = 8.23 ºC).

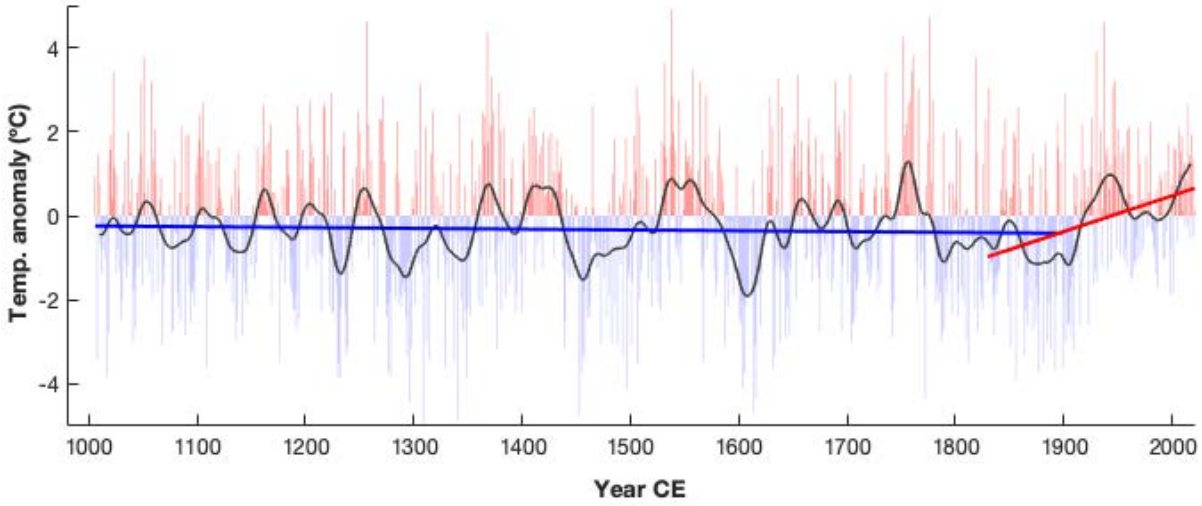

Figure 12. The updated Ammarnäs MXD based warm season (April - August) temperature reconstruction, given as anomalies relative to the 1971 – 2000 mean. Annual data shown as positive temperature anomalies in red and negative in blue, and multidecadal data by the thicker black line (smoothed by a 30-year gaussian filter). Trend lines showing a vague negative trend 1010 – 1900 CE (thick blue line) and a more pronounced positive trend 1800 – 2021 CE (thick red line).

Table 3
Temperature anomalies in relation to 1971-2000 mean, note some differences in time intervals (period).

Period	Positive	Negative	Difference
1922-2021	60	40	+20
1900-2021	68	58	+10
1900-1999	52	48	+4
1800-1899	34	66	-32
1700-1799	42	58	-16
1600-1699	39	61	-22
1500-1599	29	30	+1

4.3. Comparison in a latitudinal climate gradient

A comparison has been done between Ammarnäs and three other summer temperature reconstructions; Torneträsk and Jämtland, built on MXD data, and Rogen, which is built on blue intensity (BI) (Fig. 13 and Appendix 5 for individual comparisons). Ammarnäs seems to have most in common with the reconstruction from Jämtland (Appendix 5), while Rogen and Torneträsk partly shows similar trends. In the part of the reconstructions before 1300 CE Torneträsk is showing a different pattern compared with the tree other. Between 1300 and 1600 CE all four reconstructions are fairly similar. From 1600 – 1900 CE no homogenous pattern between the four data sets can be seen, but Jämtland and Ammarnäs are showing many similarities, while Rogen and Torneträsk shows some similarities, but not as pronounced. On the other hand, from around 1900 CE until present, the most homogenous period throughout the whole period can be seen.

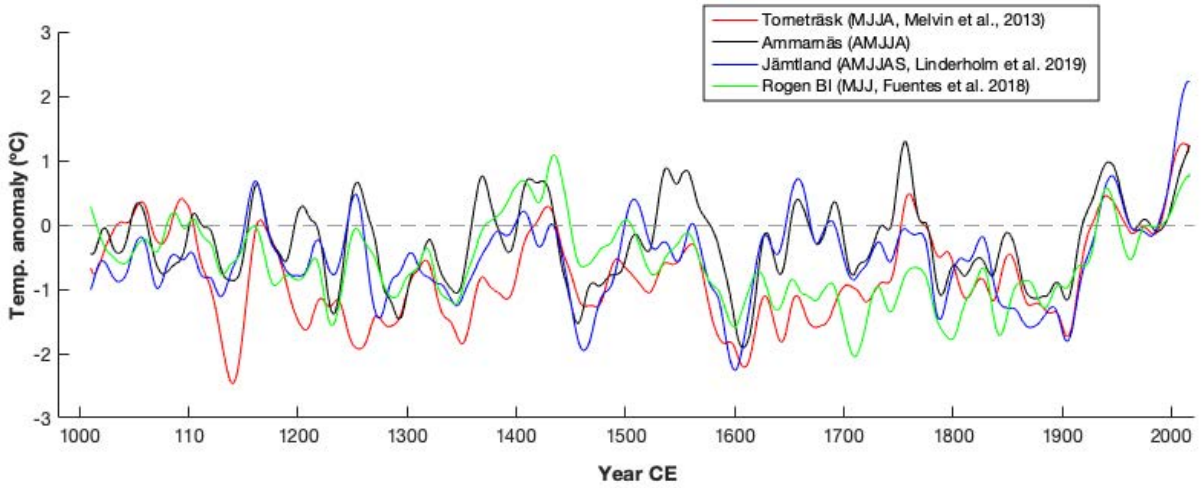

Figure 13. A comparison between Torneträsk, Ammarnäs, Jämtland and Rogen (BI). All data are given as anomalies relative to the 1971 – 2000 mean and are smoothed by a 30-year gaussian filter.

4.4. The timing of the industrial warming

The timing from pre-industrial to industrial climate in the updated Ammarnäs chronology have been investigated by preforming a change point analysis. When the analysis was performed on the MXD data from Ammarnäs the timing of the change was set to 1915 CE (Fig. 14) and for the TRW data 1913 CE. In the MXD reconstruction, the mean value for 1010 CE – 1914 CE is -0.3421 and for 1915 – 2021 CE it is 0.3693 (Fig. 14). The timing of the transition in smoothed MXD data were not showing any distinct difference in timing (smoothed 30 years 1916, 50 years 1917, 100 years 1917).

For the other three locations the timing of the change point were set to; Rogen 1929, Jämtland 1932, and Torneträsk 1916 (Fig. 15). The time of change to industrial climate are earlier in the two more northern locations, Torneträsk and Ammarnäs, than in Rogen and Jämtland, located in central Sweden.

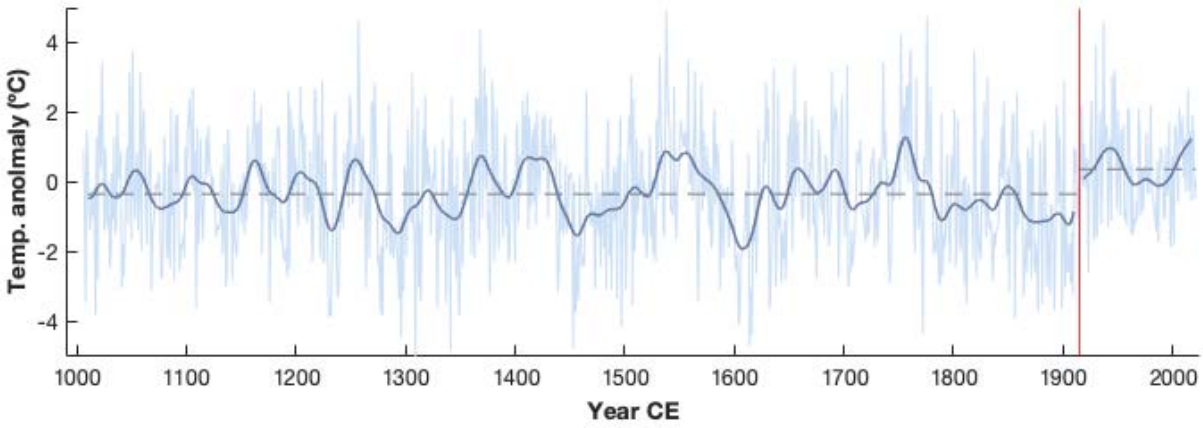

Figure 14. Change point analysis on the temperature reconstruction from Ammarnäs, given as anomalies relative to the 1971 – 2000 mean. The red line represents the calculated time of change to industrial climate (1915). The light blue line represents annual data and thicker black line 30-year smoothing by a gaussian filter. The mean values are represented by dashed lines, the mean of 1010 – 1914 CE is -0.3421 and of 1915 – 2021 CE 0.3693.

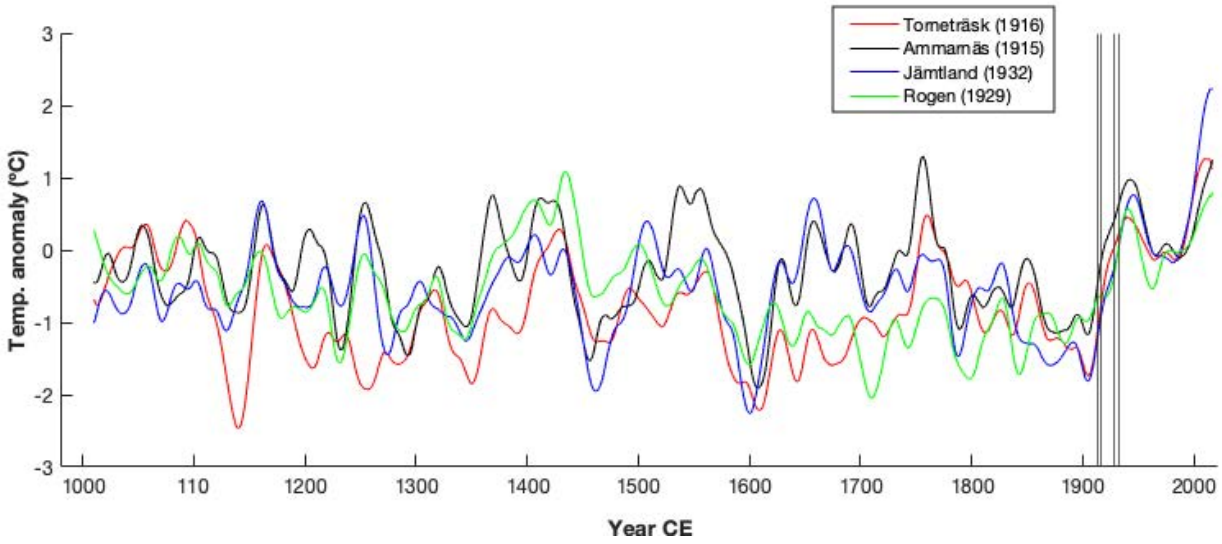

Figure 15. Change point analysis on the temperature reconstruction from Torneträsk, Ammarnäs, Jämtland and Rogen, given as anomalies relative to the 1971 – 2000 mean and 30-year smoothing by a gaussian filter. The black vertical lines represent the calculated time of change to industrial climate; 1915 (Ammarnäs), 1916 (Torneträsk), 1929 (Rogen) and 1932 (Jämtland).

5. Discussion

5.1. The updated MXD data from Ammarnäs

The aims of this thesis were to identify the timing of when the current warming started to influence the trees in the update and improve the Ammarnäs tree-ring chronologies, based on TRW and MXD data from Scots Pine. There was a wish to use multiple types of proxy data from the Arctic region, but as the MXD data did show a much stronger correlation to instrumental temperature data (Fig. 7), which have been seen in previous studies too (Gouirand et al., 2008; Ljungqvist et al., 2020), this proxy has been the main source of further analyses. The updated MXD chronology from Ammarnäs, hence forward referred to as Ammarnäs, correlated well with the instrumental record of April – August temperatures from the close lying metrological station in Stensele and a temperature reconstruction was made from the MXD data. The updated data set showed an improvement from the old data, both in its ability to explain the variance of temperature in the observed data and in time of an EPS value above the threshold 0.85. Improvements of the temperature reconstruction were expected as the data was more than doubled in the updated chronology. Furthermore, the Ammarnäs chronology could possibly, only by adding a few more samples during the right time span, be updated to become reliable back to the middle of the 14th century instead of 1511 CE, as today.

In the reconstruction from Ammarnäs the current warming can visually be seen from approximately 1900 (Fig. 11) and a change point analysis define this transition to 1915 CE (Fig. 14). The period 1900 – 2021 CE are showing the largest difference in average mean temperature in comparison to previous century, within the period 1511 – 2021 CE, and the present warming shows the highest rate of warming per decade during the same period. This agrees with the common view of an climate change unprecedented during the last 2 kyr (Masson-Delmotte et al., 2021). The 20th and 21th centuries also show a difference in distribution of warm and cold annual temperature anomalies from the used reference period (1971 – 2000), with substantively

more warm than cold annual anomalies between 1900 – 2021 (Table 3 & Fig. 12). In the rest of the reconstruction, except from the 16th century, the pattern is reversed with substantively more years of negative anomalies than positive. The period 1500 – 1599 CE shows a minor predominance of positive anomalies (+1) (Table 3).

The lack of a pronounced long-term trends in tree-ring reconstructions, due to the shortness of the proxy components (i.e., indices) and possibly as a response to the detrending method, causes a rather flat time series on a long-time scale (Esper et al., 2003; 2016). Despite this, there is a slight negative trend in the pre-industrial period compared to the industrial warming phase, which shows a more significant positive trend (Fig. 12). As the long-term trend is vague the visual indication of the current warming is not showing to much of an anormal trend in the plotted data, but with the trend lines in Fig. 12, this can more easily be seen. Together with the evidence of largest centennial-scale change in temperature compared to previous century, the unusual warming rate and the predominance of positive temperature anomalies compared to 1971 – 2000 mean (Table 3 & Fig. 12), the current warming is the most prominent and sustained change in the temperature reconstruction from Ammarnäs. This supports the conclusion that the reconstructed MXD data from Ammarnäs is showing the signal of the current global warming.

5.2. The timing of the transition to industrial climate

The three other tree-ring based temperature reconstructions that have been used for comparison, Rogen, Jämtland and Torneträsk (Fig. 13) are showing similar patterns as Ammarnäs concerning the current warming trend. The visual change to industrial climate can be seen around 1900 CE and all four data sets correlates the best from this point and onwards. To investigate the timing of when the warming can be confirmed statistically a change point analysis have been used. The timing in Ammarnäs is as mentioned, set to 1915 by this method (Fig. 14). In the other three locations the timing is fairly close, and from south to north, the change point is in Rogen 1929, Jämtland 1932, Ammarnäs 1915 and Torneträsk 1916 (Fig. 15). There are minor differences in the year of change between the sites, but earlier timings can be seen in the two more northern reconstructions than in the two southern once. This displays a possibility of an earlier shift from pre-industrial to industrial climate further north, but the result would benefit from more comparisons to see if this is a trend that are repeated in other temperature reconstructions. If this would be the case, it might indicate that the anthropogenic warming was detectable earlier further north and that the Arctic region not only shows a larger extent of warming, but also have experienced a longer period of significant anthropogenic warming.

The results of the timings are very different from what was seen in the study performed by Abram et al. (2016), where a transition to industrial climate in the Arctic region was seen already in the first half of the 19th century (in reconstruction 1831 CE and in simulation 1943 CE). The method used by Abram et al. (2016) is a more complex change point analysis, "Significant Zero crossings of derivatives" (SiZer), and a comparison to the results from this study can possibly be unsuitably to draw conclusions from. There are also differences in used data, both in used archives and spatial distribution. The difference between the result from Abram et al. and this study is almost hundred years, which is more than might be expected, which raises the question of how the data from Abram et al. would perform in an analysis by the method used in this study, and vice versa.

Further, some of the chosen locations might be unrepresentative for the Arctic region and therefore not suitable to compare to the results from Abram et al. (2016). On the other hand, the spatial coverage of significant correlation between observed warm season temperatures and the MXD data from Ammarnäs (Appendix 4) does included areas than can be included in the Arctic region by other properties than latitude (AMAP, 1998). Furthermore, this also proves the usage of Scots Pine as a proxy representing warm season temperatures of parts of the Arctic region.

The different timings of the transition to an industrial climate that have been discovered in the four locations could possibly be attributed to other site properties, such as regional geography and micro-climate, or influences from the atmospheric or oceanic circulations, such as the NAO or AMV. The used tree-ring based temperature reconstructions have been created by different investigators and differences can also occur due to sampling strategy, preparation, measurements and standardization methods, etc. (Neukom, Barboza, et al., 2019).

5.3. The influence of natural climate forcings

Natural variabilities of the climate complicate the investigation of the timing of the change from pre-industrial to industrial climate. Decadal- to multidecadal-scale variabilities between warm and cold periods can be seen throughout the temperature reconstruction, these changes are caused by internal and external forces on the climate system causing either negative (cooling) or positive (warming) effective radiative forcing (Gulev et al., 2021). Broennimann et al. (2019) concludes that the end of LIA was marked by the recovery from a sequence of volcanic eruptions and that this causes a difficulty to define a single pre-industrial baseline. It is possible that volcanic eruptions have masked some of the early induced anthropogenic warming (Fig. 16), but on the other hand, after a cool period due to volcanism, the climate usually recover by a fast-warming episode, which in this case could have caused a false indication of early warming signs.

Volcanic eruptions have influenced the climate substantively during the time period 1300 – 1900 CE (Broennimann et al., 2019; Gulev et al., 2021; Neukom, Barboza, et al., 2019), an important period when trying to define a representative period of pre-industrial temperatures. During the mid-18th century, a warming trend can be seen in all four temperature reconstructions (Fig. 13), but the warming is interrupted, possibly by large volcanic eruptions in the beginning of the 19th centaury (Fig. 16), causing temperatures to cool again. This causes the last phase of the LIA, and the recovery afterwards causes a shift into the modern warming. During the period 1750 – 1900 CE, GHG had start to rise due to human activates. Further, Hawkins. et al. (2017) and Schurer et al. (2017) argues that this would most likely have started to influence the temperature. But according to IPCC (AR6, WGI) the rise in GHG, mainly CO_2, until 1850 CE was too small to have any influence on the climate. On the other hand, the IPCC report *is* lifting the human influence on the global temperature by that time, but as the uncertainties are too large, they have chosen to not take this in consideration when choosing their arbitrary pre-industrial baseline (Chen et al., 2021).

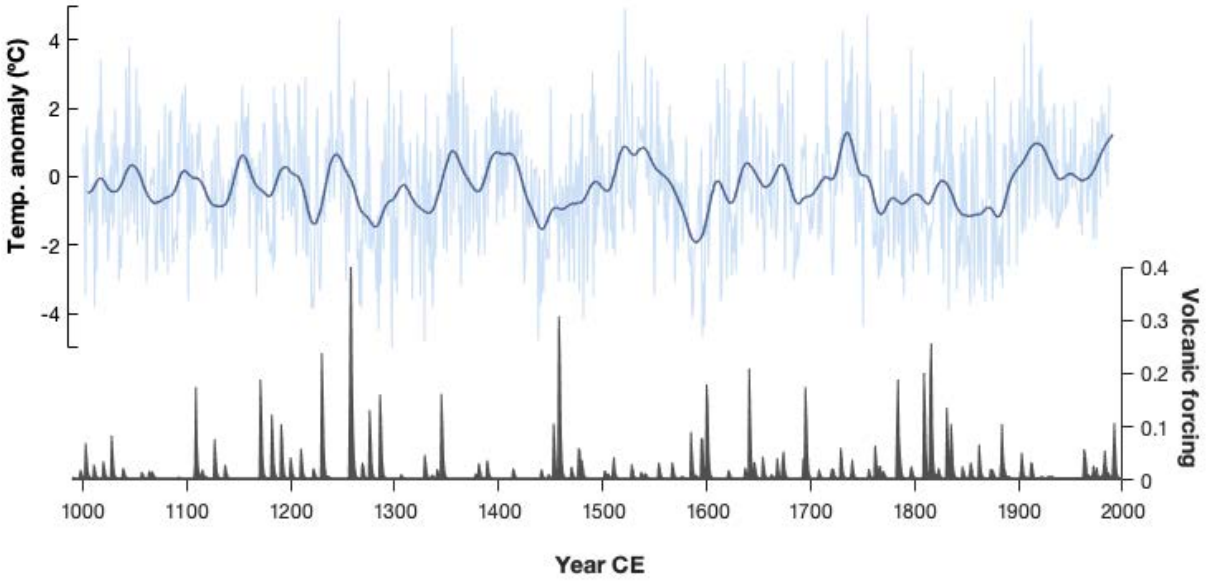

Figure 16. Temperature reconstruction from Ammarnäs MXD data, anomalies from 1971-2000 mean, annual and 30-year smoothing by a gaussian filter. Volcanic forcing showing the aerosol optical depth (AOD) (Neukom, Barboza, et al., 2019).

5.4. A regional approach to a pre-industrial baseline

To be able to meet goals set to limiting the human caused global warming there might be a good reason to define the pre-industrial as a baseline which is, with the greatest probability, not effected by human caused global warming. A suitable period to use for this have been proposed by Hawkins et al. (2017) to be 1720 – 1800 CE, but according to Schurer et al. (2017), the pre-industrial should preferably be defined to even be before 1750 CE, to avoid human influences on the climate system.

The transition from pre-industrial to industrial climate might not be suitable to be set as a point from pre-industrial to industrial climate, but rather as a time of change compared to a base from further back in time, representing pre-industrial temperature values. This baseline would preferably be before 1750 if it should not be influenced by the enhanced amounts of CO_2 in the atmosphere from burning of fossil carbon (Schurer et al., 2017).

Even if the timing of the change in this study is after 1900 CE, the transitions are detected in the early 20th century and earlier in the more northern parts. This could be a trend, with even earlier transitions times further north, indicating that a pre-industrial baseline would benefit from being set to an earlier time, than 1850 – 1900 CE, if looking for a period without the influence from human caused warming. The study from Abram et al. (2016) does show that within this more synchronous warming period of the present, regionally differences of significance does occur. This strongly suggests that regional differences must be sufficiently investigated when approaching the question of the timing from pre-industrial to industrial climate and that global simulations with areas like the Arctic left out might not be suitable when choosing the period of a pre-industrial temperature reference (Hawkins et al., 2017; Schurer et al., 2018).

6. Conclusion

The updated TRW and MXD chronologies from Ammarnäs were statistically improved and extended from 1277 CE to 1010 CE. They correlated to varying extent with the instrumental record from the close lying metrological station in Stensele. The MXD data showed a profoundly better correlation than TRW, and the April - August temperature reconstruction based on MXD data was used for further analyses. The updated MXD chronology showed an improvement from the old data, both in its ability to explain the variance of temperature in the observed data and in time of an EPS value above the threshold 0.85.

The current warming was statistically detectable in the MXD based temperature reconstruction. It was proven by a higher rate of warming than seen in any other part of the chronology, with a predominance of positive temperature anomalies compared to 1971 – 2000 mean and a vague long-term cooling trend of the pre-industrial period, interrupted by a significant warming trend of the industrial era.

The results from preformed change point analyses, on the four tree-ring reconstructions of warm season temperatures from the central to northern of Sweden, does not indicate a timing of the transition from pre-industrial to industrial climate that interferes with the pre-industrial baseline (1850 – 1900 CE) defined by IPCC (AR6, WGI). On the other hand, the points of change to an industrial climate were all in the first half of the 20th century (1915, 1916, 1929 and 1932) and further north, the transition were seen earlier.

Further research is needed to investigate the question of a possible earlier transition from preindustrial to industrial climate in the Arctic region. This might give results that are questioning the usage of 1850 – 1900 CE as an arbitrary baseline of pre-industrial levels of temperature, such as IPCC does. This question is of major interest as the pre-industrial baseline is used as a reference in climate goalsetting and mitigations, and therefore of importance to be defined to a period with minor human influences on the climate system.

7. Suggestion on further work and improvements

There are some possible improvements that can be done on the chronology. The samples collected in 2021 were taken in different elevations, these showed some difference in correlation to the temperature data. Adjustments accordingly were explored, but no adjustment was done as more time was needed to find the best option. Furthermore, the new data was correlating better to the observed temperature data than the old, and some adjustments might be possible to strengthen the correlation and explained variance to the instrumental data used in the temperature reconstruction. These adjustments can and should be scientifically motivated, as e.g. exclude sites below a certain elevation as temperature is better correlated closer to the treeline, to avid cherry picking.

There is an agreement to the hypothesis of an earlier transition to industrial climate in the locations furthest north in this study, but this must be further investigated to be proven. Still, the results show that it is possible and here follows some suggestion on improvements of the method.

Tree-rings often correlates well with growing season temperatures. This is a little unfortune as the temperatures in the study region are more affected during the winter by the current warming. Furthermore, as the AA is larger during the winter, it is possible that other archives might show other results. To have more than one archive and multiple proxies would have been benefiting for the relatability of the results.

The study area, the central to northern of Sweden, could be included in the arctic region if defined as 60 – 90 ºN. However, with the hypothesis of the AA and an earlier onset of the warming in mind, it would be interesting to use data from archives further north. A latitudinal transection has been used in this study, it would also be interesting to expand the study area further in longitude (possibly comparing result in longitudinal bands), to improve the spatial distribution over the Arctic region. A southern reference would also be benefiting.

Only four data sets have been used in this study to define the result, a higher replication of used data sets would be benefitting, this could improv the reliability of the result substantively.

The method used to decide the timing of the transition, the change point analysis, could be further explored and possibly developed to better fit the study. As mentioned in a previous part, the method (SiZer analysis) and data used by Abram et al. (2016) would be interesting to compare with the data in this study and additional data too.

Acknowledgement

I would like to start with to send a large thank to my supervisor Hans Linderholm for all your help, support and encouragement. Thank you for giving me so much new knowledge and for all guidance you have provided me through this process. It has also been helpful to hear your old stories of sleep deprivation due to small kids at home etc., it made me feel that I could manage it too.

I also would like to thank Björn Gunnarsson for letting me in to "your" lab, generously devote you time to show me the technique of MXD measurement and for letting me use the existing Ammarnäs chronology. I really enjoyed my time at Stockholm University, thank you Björn.

Mauricio Fuentes, you have been a large help to me and a source to joy in the lab. Thank you for all your sketches and long explanations.

I also like to thank Fredrik Karlsson, who I spent many hours together with in the lab. Some days we did say nothing, other we talked a lot, but I always enjoyed your company. All questions I did not dare to ask anyone else, I felt safe to ask you. Thank you for all your help and support, it would have been much harder and lonelier without you. I am happy we wrote our master thesis at the same time and I wish you all luck with future adventures.

I don't know what I should have done without Petter Stridbeck, thank you for introducing me to MatLab, it has been priceless to me.

Further, thank you Jesper Björklund and Kristina Seftingen, and the GULD community, for always being helpful and welcoming.

On my field trip, there are several people who opened their home for us, wet and miserable (some days) campers. Thank you, Tina and Jonas Petterson, for being so hospitable and for letting us sleep well, and long, after many nights in the tent with a baby. Thank you Jenny and Sara Råghall, for letting us dry up and manage to store all collected samples.

Finally, all my love and largest thank goes to my family. Thank you, Oscar, for always supporting me and letting me work way very much in some periods. I know that you always take the best care of our little Sigge. The two of you were always in my mind, my best partners in life and as assistants in field. I would also like to thank you Ann-Marie Falkensjö, my mother, and Sigge's grandmother. Your support as "Bobbo" has been priceless and very joyful to us.

References

Abram, N. J., McGregor, H. V., Tierney, J. E., Evans, M. N., McKay, N. P., Kaufman, D. S., Thirumalai, K., Martrat, B., Goosse, H., Phipps, S. J., Steig, E. J., Kilbourne, K. H., Saenger, C. P., Zinke, J., Leduc, G., Addison, J. A., Mortyn, P. G., Seidenkrantz, M.-S., Sicre, M.-A., . . . Von Gunten, L. (2016). Early onset of industrial-era warming across the oceans and continents. *Nature (London)*, *536*(7617), 411-418. https://doi.org/10.1038/nature19082

Allen, M. R., O.P. Dube, W. Solecki, F. Aragón-Durand, W. Cramer, S., Humphreys, M., Kainuma, J. K., N. Mahowald, Y. Mulugetta, R. Perez, M. Wairiu, & K. Zickfeld. (2018). Framing and Context. In: Global Warming of 1.5°C. An IPCC Special Report on the impacts of global warming of 1.5°C above pre-industrial levels and related global greenhouse gas emission pathways, in the context of strengthening the global response to the threat of climate change, sustainable development, and efforts to eradicate poverty [Masson-Delmotte, V., P. Zhai, H.-O. Pörtner, D. Roberts, J. Skea, P.R. Shukla, A. Pirani, W. Moufouma-Okia, C. Péan, R. Pidcock, S. Connors, J.B.R. Matthews, Y. Chen, X. Zhou, M.I. Gomis, E. Lonnoy, T. Maycock, M. Tignor, and T. Waterfield (eds.)].]. *In Press*.

AMAP. (1998). Physical/Geographical Characteristics
of the Arctic. *Chapter 2*, 10 - 24 pp.

AMAP. (2017). Snow, Water, Ice and Permafrost in the Arctic (SWIPA) 2017. . xiv + 269 pp.

AMAP. (2021). Arctic Climate Change Update 2021: Key Trends and Impacts. Summary for Policy-makers. *Arctic Monitoring and Assessment Programme (AMAP).*(Tromsø, Norway.), 16 pp.

AMAP. (2022). *Geographical coverage*. https://www.amap.no/about/geographical-coverage

Aminikhanghahi, S., & Cook, D. J. (2016). A survey of methods for time series change point detection. *Knowledge and information systems*, *51*(2), 339-367. https://doi.org/10.1007/s10115-016-0987-z

Bindoff, N. L., Cheung., W. W. L., J.G. Kairo, J. Arístegui, V.A. Guinder, R. Hallberg, N. Hilmi, N. Jiao, M.S. Karim, L. Levin, S. O'Donoghue, S.R. Purca Cuicapusa, B. Rinkevich, T. Suga, Tagliabue, A., & Williamson, P. (2019). Changing Ocean, Marine Ecosystems, and Dependent Communities. In: IPCC Special Report on the Ocean and Cryosphere in a Changing Climate [[H.-O. Pörtner, D.C. Roberts, V. Masson-Delmotte, P. Zhai, M. Tignor, E. Poloczanska, K. Mintenbeck, A. Alegría, M. Nicolai, A. Okem, J. Petzold, B. Rama, N.M. Weyer (eds.)].]. *Cambridge University Press, Cambridge, UK and New York, NY, USA.*, pp. 447-587. https://doi.org/https://doi.org/10.1017/9781009157964.007.

Broennimann, S., Franke, J., Nussbaumer, S. U., Zumbuhl, H. J., Steiner, D., Trachsel, M., Hegerl, G. C., Schurer, A., Worni, M., Malik, A., Flueckiger, J., & Raible, C. C. (2019). Last phase of the Little Ice Age forced by volcanic eruptions. *Nature geoscience*, *12*(8), 650-656. https://doi.org/10.1038/s41561-019-0402-y

Chen, D., Rojas, M., Samset, B. H., Cobb, K., Diongue Niang, A., Edwards, P., Emori, S., Faria, S. H., Hawkins, E., Hope, P., Huybrechts, P., Meinshausen, M., Mustafa, S. K., Plattner, G. K., & Tréguier, A. M. (2021). Framing, Context, and Methods. In V. Masson-Delmotte, P. Zhai, A. Pirani, S. L. Connors, C. Péan, S. Berger, N. Caud, Y. Chen, L. Goldfarb, M. I. Gomis, M. Huang, K. Leitzell, E. Lonnoy, J. B. R. Matthews, T. K. Maycock, T. Waterfield, O. Yelekçi, R. Yu, & B. Zhou (Eds.), *Climate Change 2021: The Physical Science Basis. Contribution of Working Group I to the Sixth Assessment Report of the Intergovernmental Panel on Climate Change* (pp. 147–286). Cambridge University Press. https://doi.org/10.1017/9781009157896.003

Cook, E., Krusic, P., & Melvin, T. (2014). Program RCSsigFree: Version 45_v2b. *Lamont-Doherty Earth Obs. Columbia University*.

Cook, E. R., Meko, D. M., Stahle, D. W., & Cleaveland, M. K. (1999). Drought Reconstructions for the Continental United States. *Journal of climate*, *12*(4), 1145-1162. https://doi.org/10.1175/1520-0442(1999)012<1145:drftcu>2.0.co
2

Crowley, T. J., & Unterman, M. B. (2013). Technical details concerning development of a 1200 yr proxy index for global volcanism. *Earth system science data*, *5*(1), 187-197. https://doi.org/10.5194/essd-5-187-2013

Esper, J., Cook, E. R., Krusic, P. J., Peters, K., & Schweingruber, F. H. (2003). Tests of the RCS method for preserving low-frequency variability in long tree-ring chronologies. *Tree-ring research*, *59*(2), 81-98.

Esper, J., Krusic, P. J., Ljungqvist, F. C., Luterbacher, J., Carrer, M., Cook, E., Davi, N. K., Hartl-Meier, C., Kirdyanov, A., Konter, O., Myglan, V., Timonen, M., Treydte, K., Trouet, V., Villalba, R., Yang, B., & Buentgen, U. (2016). Ranking of tree-ring based temperature reconstructions of the past millennium. *Quaternary Science Reviews*, *145*, 134-151. https://doi.org/10.1016/j.quascirev.2016.05.009

Fritts, H. C. (1976). *Tree rings and climate*. London : Academic Press.

Gouirand, I., Linderholm, H. W., Moberg, A., & Wohlfarth, B. (2008). On the spatiotemporal characteristics of Fennoscandian tree-ring based summer temperature reconstructions. *Theoretical And Applied Climatology, 2008, Vol. 91, Iss. 1-4, pp. 1-.25*, *91*(1-4), 1-25.

Gulev, S. K., Thorne, P. W., Ahn, J., Dentener, F. J., Domingues, C. M., Gerland, S., Gong, D., Kaufman, D. S., Nnamchi, H. C., Quaas, J., Rivera, J. A., Sathyendranath, S., Smith, S. L., Trewin, B., von Schuckmann, K., & Vose, R. S. (2021). Changing State of the Climate System. In V. Masson-Delmotte, P. Zhai, A. Pirani, S. L. Connors, C. Péan, S. Berger, N. Caud, Y. Chen, L. Goldfarb, M. I. Gomis, M. Huang, K. Leitzell, E. Lonnoy, J. B. R. Matthews, T. K. Maycock, T. Waterfield, O. Yelekçi, R. Yu, & B. Zhou (Eds.), *Climate Change 2021: The Physical Science Basis. Contribution of Working Group I to the Sixth Assessment Report of the Intergovernmental Panel on Climate Change* (pp. 287–422). Cambridge University Press. https://doi.org/10.1017/9781009157896.004

Hawkins, E., Ortega, P., Suckling, E., Schurer, A., Hegerl, G., Jones, P., Joshi, M., Osborn, T. J., Masson-Delmotte, V., Mignot, J., Thorne, P., & Van Oldenborgh, G. J. (2017). ESTIMATING CHANGES IN GLOBAL TEMPERATURE SINCE THE PREINDUSTRIAL PERIOD. *Bulletin of the American Meteorological Society*, *98*(9), 1841-1856. https://doi.org/10.1175/BAMS-D-16-0007.1

Hawkins., Suckling, E., Ortega, P., Schurer, A., Hegerl, G., Jones, P., Joshi, M., Osborn, T. J., Masson-Delmotte, V., Mignot, J., Thorne, P., & van Oldenborgh, G. J. (2017). Estimating Changes in Global Temperature since the Preindustrial Period. *Bulletin of the American Meteorological Society*, *98*(9), 1841-1856. https://doi.org/10.1175/bams-d-16-0007.1

Helama, S., Lindholm, M., Timonen, M., & Eronen, M. (2004). Detection of climate signal in dendrochronological data analysis: a comparison of tree-ring standardization methods. *Theoretical and applied climatology*, *79*(3), 239-254. https://doi.org/10.1007/s00704-004-0077-0

Holmes, R. L. (1983). Computer-Assisted Quality Control in Tree-Ring Dating and Measurement. http://hdl.handle.net/10150/261223

Hurrell, J. W., Kushnir, Y., & Visbeck, M. (2001). The North Atlantic oscillation. *Science (American Association for the Advancement of Science)*, *291*(5504), 603, 605-605. https://doi.org/10.1126/science.1058761

Kaufman, D. S., Schneider, D. P., McKay, N. P., Ammann, C. M., Bradley, R. S., Briffa, K. R., Miller, G. H., Otto-Bliesner, B. L., Overpeck, J. T., Vinther, B. M., Abbott, M., Axford, Y., Bird, B., Birks, H. J. B., Bjune, A. E., Briner, J., Cook, T., Chipman, M., Francus, P., . . . Thomas, E. (2009). Recent warming reverses long-term Arctic cooling. *Science (American Association for the Advancement of Science)*, *325*(5945), 1236-1239. https://doi.org/10.1126/science.1173983

Linderholm, H. W., Folland, C. K., & Hurrell, J. (2008). Reconstructing Summer North Atlantic Oscillation (SNAO) variability over the last five centuries. *Tree Rings In Archaeology, Climatology And Ecology, 2008, Vol. 6, pp. 8-.16*, *6*, 8-16.

Linderholm, H. W., Folland, C. K., & Walther, A. (2009). A multicentury perspective on the summer North Atlantic Oscillation (SNAO) and drought in the eastern Atlantic region. *Journal of quaternary science*, *24*(5), 415-425. https://doi.org/10.1002/jqs.1261

Linderholm, H. W., & Gunnarson, B. E. (2019). Were medieval warm-season temperatures in Jämtland, central Scandinavian Mountains, lower than previously estimated? *Dendrochronologia (Verona)*, *57*(October), 125607. https://doi.org/10.1016/j.dendro.2019.125607

Linderholm, H. W., Gunnarson, B. E., & Liu, Y. (2010). Comparing Scots pine tree-ring proxies and detrending methods among sites in Jämtland, west-central Scandinavia. *Dendrochronologia, 2010, Vol. 28, Iss. 4, pp. 239-.249*, *28*(4), 239-249.

Linderholm, H. W., Zhang, P., Gunnarson, B., Björklund, J., Farahat, E., Fuentes, M., Rocha, E., Salo, R., Seftigen, K., Stridbeck, P., & Liu, Y. (2014). Growth dynamics of tree-line and lake-shore Scots pine (Pinus sylvestris L.) in the central Scandinavian Mountains during the Medieval Climate Anomaly and the early Little Ice Age. *Frontiers In Ecology And Evolution, 2014, Vol. 2*, *2*.

Ljungqvist, F. C., Thejll, P., Björklund, J., Gunnarson, B. E., Piermattei, A., Rydval, M., Seftigen, K., Støve, B., & Büntgen, U. (2020). Assessing non-linearity in European temperature-sensitive tree-ring data. *Dendrochronologia (Verona)*, *59*, 125652. https://doi.org/10.1016/j.dendro.2019.125652

Masson-Delmotte, V., Schulz, M., Abe-Ouchi, A., Beer, J., Ganopolski, A., González Rouco, J. F., Jansen, E., Lambeck, K., Luterbacher, J., Naish, T., Osborn, T., Otto-Bliesner, B., Quinn, T., Ramesh, R., Rojas, M., Shao, X., & Timmermann, A. (2013). Information from Paleoclimate Archives. In T. F. Stocker, D. Qin, G.-K. Plattner, M. Tignor, S. K. Allen, J. Boschung, A. Nauels, Y. Xia, V. Bex, & P. M. Midgley (Eds.), *Climate Change 2013: The Physical Science Basis. Contribution of Working Group I to the Fifth Assessment Report of the Intergovernmental Panel on Climate Change* (pp. 383–464). Cambridge University Press. https://doi.org/10.1017/CBO9781107415324.013

Masson-Delmotte, V., Zhai, P., Pirani, A., Connors, S. L., Péan, C., Berger, S., Caud, N., Chen, Y., Goldfarb, L., Gomis, M. I., Huang, M., Leitzell, K., Lonnoy, E., Matthews, J. B. R., Maycock, T. K., Waterfield, T., Yelekçi, O., Yu, R., & Zhou, B. (2021). *IPCC, 2021: Climate Change 2021: The Physical Science Basis. Contribution of Working Group I to the Sixth*. C. U. Press.

MathWorks. (2022). *Find abrupt changes in signal, "findchnagepts"*. https://se.mathworks.com/help/signal/ref/findchangepts.html

McKay, N. P., & Kaufman, D. S. (2014). An extended Arctic proxy temperature database for the past 2,000 years. *Scientific data*, *1*(1), 140026-140026. https://doi.org/10.1038/sdata.2014.26

Melvin, T. M., & Briffa, K. R. (2008). A "signal-free" approach to dendroclimatic standardisation. *Dendrochronologia (Verona)*, *26*(2), 71-86. https://doi.org/10.1016/j.dendro.2007.12.001

Meredith, M., M. Sommerkorn, S. Cassotta, C. Derksen, A. Ekaykin, A. Hollowed, G. Kofinas, A. Mackintosh, J. Melbourne-Thomas, M.M.C. Muelbert, G. Ottersen, H. Pritchard, and E.A.G. Schuur. (2019). *Polar Regions. In: IPCC Special Report on the Ocean and Cryosphere in a Changing Climate.* [H.-O. Pörtner, D.C. Roberts, V. Masson-Delmotte, P. Zhai, M. Tignor, E. Poloczanska, K. Mintenbeck, A. Alegría, M. Nicolai, A. Okem, J. Petzold, B. Rama, N.M. Weyer (eds.)]. Cambridge University Press, Cambridge, UK and New York, NY, USA, pp. 203–320. https://doi.org/https://doi.org/10.1017/9781009157964.005.

National_Research_Council. (2006). *Surface temperature reconstructions for the last 2,000 years*. Washington, D.C: National Academies Press. https://doi.org/10.17226/11676

Neukom, R., Barboza, L. A., Erb, M. P., Shi, F., Emile-Geay, J., Evans, M. N., Franke, J., Kaufman, D. S., Luecke, L., Rehfeld, K., Schurer, A., Zhu, F., Broennimann, S., Hakim, G. J., Henley, B. J., Ljungqvist, F. C., McKay, N., Valler, V., & Von Gunten, L. (2019). Consistent multidecadal variability in global temperature reconstructions and simulations over the Common Era. *Nature geoscience*, *12*(8), 643-649. https://doi.org/10.1038/s41561-019-0400-0

Neukom, R., Steiger, N., Gómez-Navarro, J. J., Wang, J., & Werner, J. P. (2019). No evidence for globally coherent warm and cold periods over the preindustrial Common Era. *Nature (London)*, *571*(7766), 550-554. https://doi.org/10.1038/s41586-019-1401-2

NOAA. (2022). *Trends in Atmospheric Carbon Dioxide*. NOAA, Global Monitoring Laboratory, Earth System Research Laboratories. https://gml.noaa.gov/ccgg/trends/monthly.html

PAGES2k. (2022). *Past Global Changes (PAST) 2k Consortium* https://pastglobalchanges.org/

Rhein, M., Rintoul, S. R., Aoki, S., Campos, E., Chambers, D., Feely, R. A., Gulev, S., Johnson, G. C., Josey, S. A., Kostianoy, A., Mauritzen, C., Roemmich, D., Talley, L. D., & Wang, F. (2013). Observations: Ocean. In T. F. Stocker, D. Qin, G.-K. Plattner, M. Tignor, S. K. Allen, J. Boschung, A. Nauels, Y. Xia, V. Bex, & P. M. Midgley (Eds.), *Climate Change 2013: The Physical Science Basis. Contribution of Working Group I to the Fifth Assessment Report of the Intergovernmental Panel on Climate Change* (pp. 255–316). Cambridge University Press. https://doi.org/10.1017/CBO9781107415324.010

Ruddiman, W. F. (2014). *Earth's climate : past and future*. New York : Freeman.

Schurer, A. P., Cowtan, K., Hawkins, E., Mann, M. E., Scott, V., & Tett, S. F. B. (2018). Interpretations of the Paris climate target. *Nature geoscience*, *11*(4), 220-221. https://doi.org/10.1038/s41561-018-0086-8

Schurer, A. P., Mann, M. E., Hawkins, E., Tett, S. F. B., & Hegerl, G. C. (2017). Importance of the pre-industrial baseline for likelihood of exceeding Paris goals. *Nature climate change*, *7*(8), 563-567. https://doi.org/10.1038/NCLIMATE3345

SMHI. (2022a). *Dataserier med normalvärden för perioden 1991-2020*. https://www.smhi.se/data/meteorologi/dataserier-med-normalvarden-for-perioden-1991-2020-1.167775

SMHI. (2022b). *Kunskapsbanken: vad är normalperioder?* https://www.smhi.se/kunskapsbanken/klimat/normaler/vad-ar-normalperioder-1.4087

Speer, J. H. (2010). *Fundamentals of tree-ring research*. Tucson, AZ : University of Arizona Press.

St John, K., Leckie, R. M., Pound, K., Jones, M., & Krissek, L. (2012). *Reconstructing earth's climate history inquiry-based exercises for lab and class* (2nd ed.). Hoboken : John Wiley & Sons.

Steinhilber, F., Abreu, J. A., Beer, J., Brunner, I., Christl, M., Fischer, H., Heikkila, U., Kubik, P. W., Mann, M., McCracken, K. G., Miller, H., Miyahara, H., Oerter, H., & Wilhelms, F. (2012). 9,400 years of cosmic radiation and solar activity from ice cores and tree rings. *Proceedings of the National Academy of Sciences - PNAS*, *109*(16), 5967-5971. https://doi.org/10.1073/pnas.1118965109

Stokes, M. A., & Smiley, T. L. (1996). *An introduction to tree-ring dating*. Tucson : University of Arizona Press.

Wanner, H., Brönnimann, S., Casty, C., Gyalistras, D., Luterbacher, J., Schmutz, C., Stephenson, D. B., & Xoplaki, E. (2001). North Atlantic oscillation - Concepts and studies. *Surveys in geophysics*, *22*(4), 321-381. https://doi.org/10.1023/A:1014217317898

Wigley, T. M. L., Briffa, K. R., & Jones, P. D. (1984). On the average value of correlated time series with applications in dendroclimatology and hydrometeorology. *Journal of Climate & Applied Meteorology*, *23*(2), 201-213. https://doi.org/10.1175/1520-0450(1984)023<0201:OTAVOC>2.0.CO
2

WMO. (2022). *WMO Climatological Normals*. https://community.wmo.int/wmo-climatological-normals

Yang, B., Qin, C., Wang, J., He, M., Melvin, T. M., Osborn, T. J., & Briffa, K. R. (2014). A 3,500-year tree-ring record of annual precipitation on the northeastern Tibetan Plateau. *Proceedings of the National Academy of Sciences - PNAS*, *111*(8), 2903-2908. https://doi.org/10.1073/pnas.1319238111

Appendix

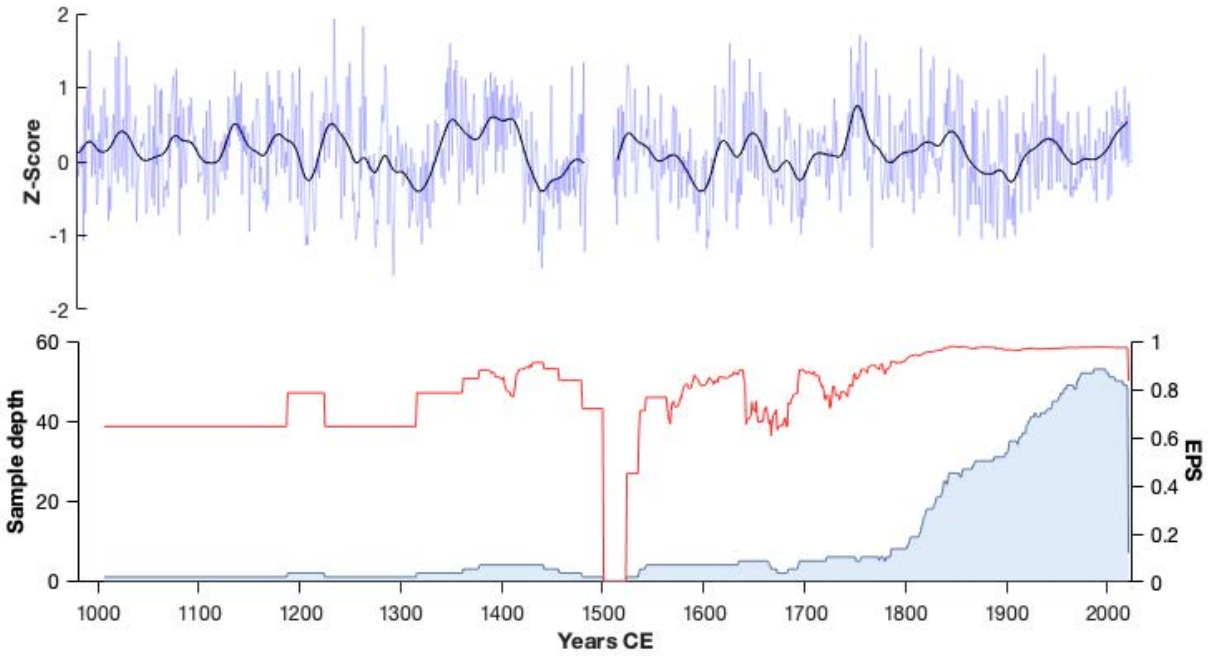

Appendix 1. Normalized values over the full period of the new samples (collected 2021) of MXD data, displayed as annual and multidecadal variability (smoothed by a 30-year gaussian filter). Sample depth and EPS can be seen in the lower part.

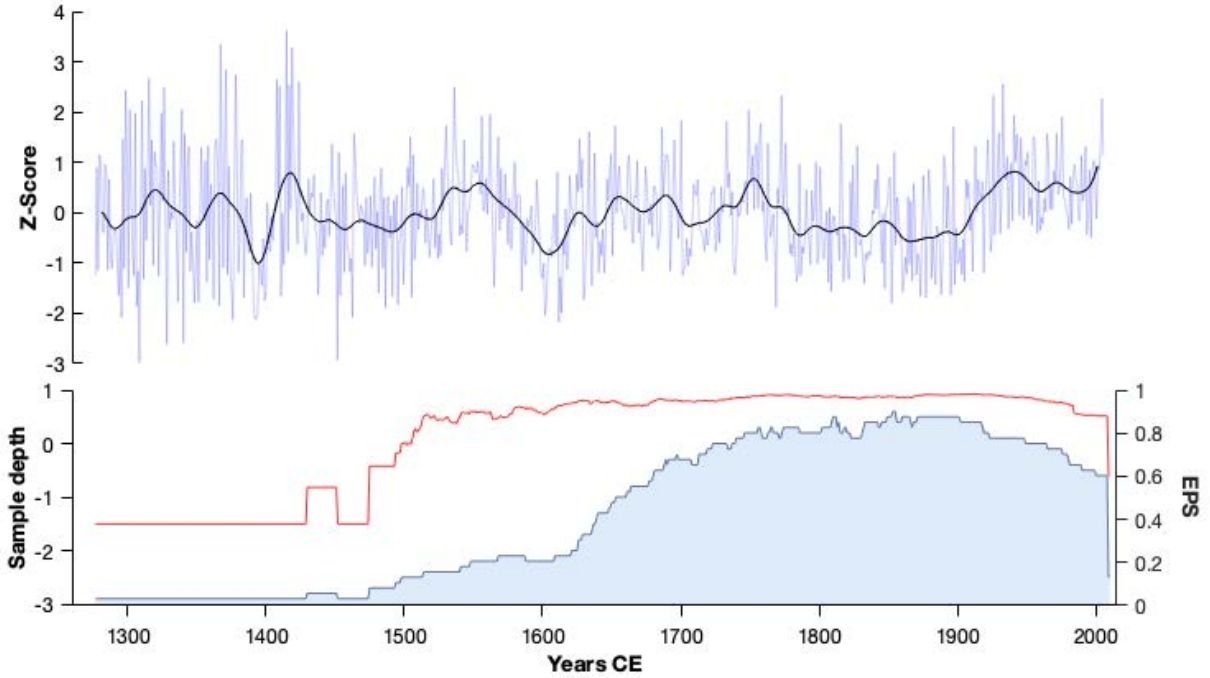

Appendix 2. Normalized values over the full period of the old samples (collected 2010) of MXD data, displayed as annual and multidecadal variability (smoothed by a 30-year gaussian filter). Sample depth and EPS can be seen in the lower part.

	New MXD data SSF chronology			Old MXD data SSFchronology		
Calibration period	1861-1932	1933-2004	1861-2004	1861-1932	1933-2004	1861-2004
Correlation, *R*	0.80*	0.71*	0.78*	0.75*	0.61*	0.72*
Explained variance, R^2	0.64	0.51	0.61	0.56	0.38	0.51
Observations	72	72	144	72	72	144
Verification period	1933-2004	1861-1932		1933-2004	1861-1932	
Explained variance, R^2	0.51	0.64		0.38	0.56	
Reduction of error, *RE*	0.60	0.69		0.51	0.63	
Coefficient of efficiency, CE	0.46	0.60		0.33	0.53	
Mean square error, MSE	0.42	0.41		0.52	0.48	
Sign test +/-	60/10	58/13		62/8	57/14	

*****Correlation is significant at the p < 0:01 level*

Appendix 3. Table of calibration and verification statistics of the April – August temperature reconstructions from the new and old MXD data from Ammarnäs.

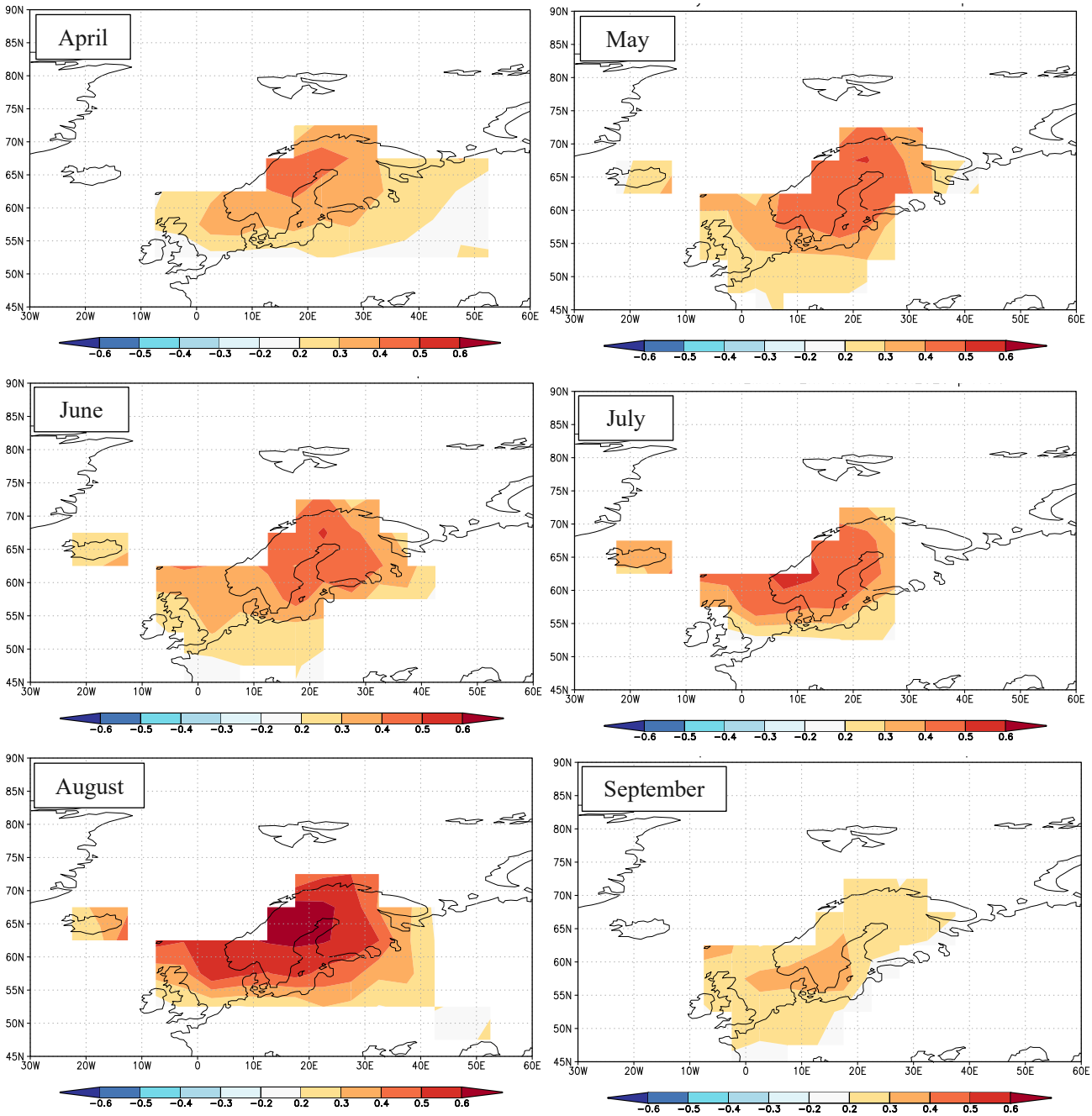

Appendix 4. Montly correlation (April – September) between gridded temperature data from CRUTEM 4.6 and MXD data from Ammarnäs, period 1850 – 2020. All month correlates significant at the $p < 0.1$ level.

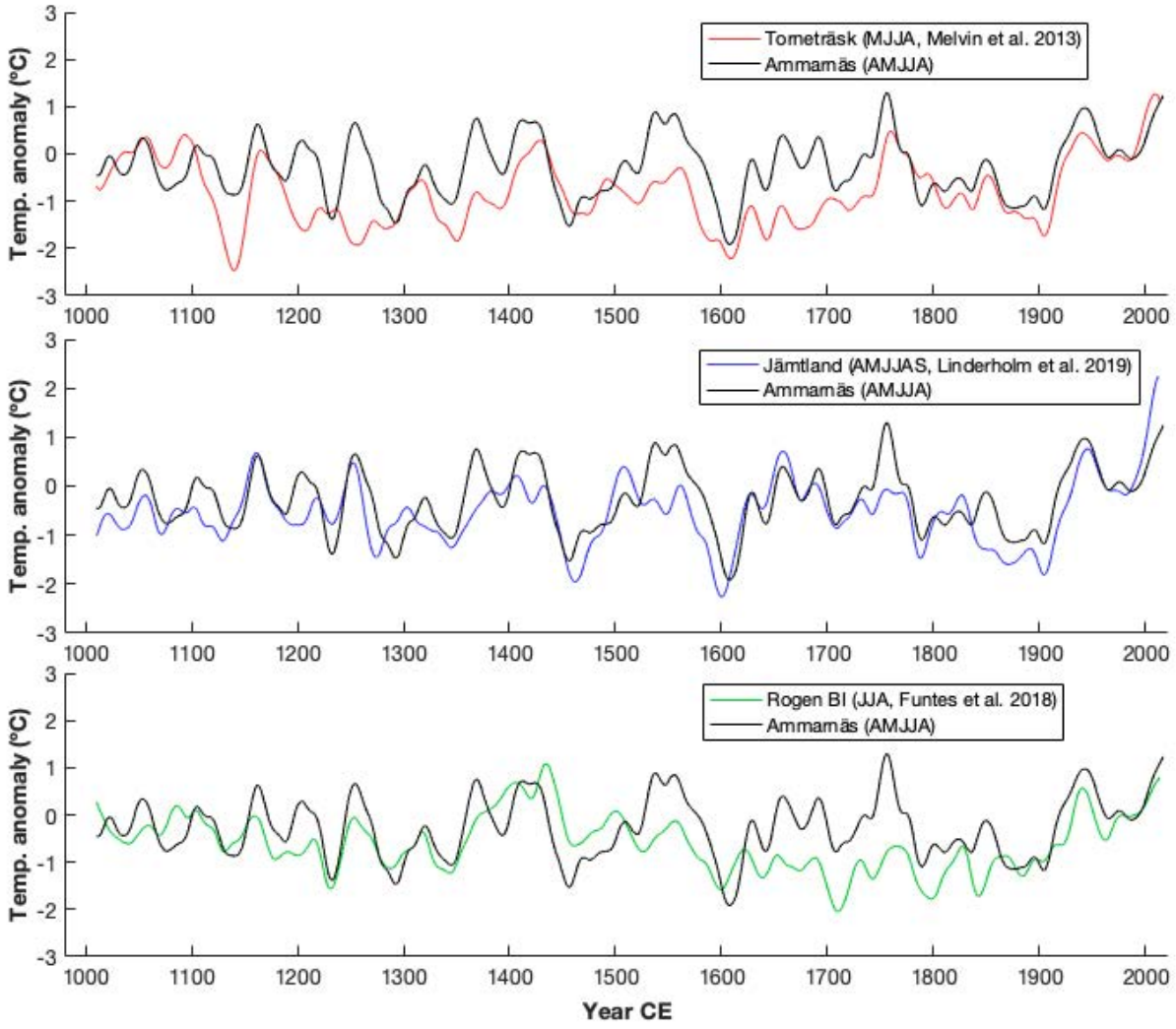

Appendix 5. Individual comparison of Ammarnäs and Torneträsk, Jämtland and Rogen. All data are given as anomalies relative to the 1971 – 2000 mean and are smoothed by a 30-year gaussian filter.